Anonymous Referee #1

REVIEWER:

General comment:

The manuscript describes dedicated experiment designed to investigate different phenomena influencing rainfall retrieval from microwave links. Several microwave links were installed over same path and equipped with time lapsed cameras shooting antenna surfaces and the link path. In addition, array of disdrometers completed with rain gauges were placed along the link path. Finally, additional observations form nearby weather station such as temperature, humidity or wind speed were used to interpret phenomena occurring during the measurement campaign. The manuscript goal is to provide comprehensive overview of different phenomena causing attenuation of microwave links and evaluate their relevance for rainfall intensity retrieval, specifically to the rainfall retrieval algorithm as suggested by Overeem et al. (2011 and 2016). The first goal is scientifically relevant as i) it might improve understanding of uncertainties affecting microwave link rainfall retrieval and ii) description of attenuation patterns from other phenomena than rainfall is crucial for improving baseline separation algorithms. The presented experimental setup is very well suited to provide reliable dataset to reach this goal. The second goal is bit too specific to the selected processing algorithms (Overeem et al. 2011 and 2016).

RESPONSE: We thank the reviewer for the positive assessment of our paper. We acknowledge that the second stated goal is too specific and this does not in fact reflect our actual intentions. The mention of the algorithms of Overeem et al (2011 and 2016) is intended merely as an example of possible integration in existing retrieval schemes and not as a goal for this paper. The text as written in P2L27-29 does not properly reflect this and we will revise it.

REVIEWER: *The manuscript focuses on describing different phenomena causing link attenuationon several selected events. Overall statistical evaluation is mostly not provided which hinders quantitative assessment of the influence of these phenomena on microwave link rainfall retrieval. Results are often presented qualitatively in subjective manner (e.g. 'link is remarkably stable') even in cases where it could be easily described quantitatively, for more details see specific comments.*

RESPONSE: We agree with the reviewer that many specific instances can be easily described more quantitatively and we will do so in the revised manuscript. Please see our resposes to the specific comments for more details.

REVIEWER: *Authors should distinguish in the whole result section more properly if the attenuation occurs along the link path or if it is rather related to hardware of microwave link radio units/antennas. The ambiguous cases should be then properly discussed and possibly confronted with radio wave propagation theory or results of other studies.*

RESPONSE: We will add clarification to the different parts of the results section where applicable. The ambiguous cases are mostly illustrative and a more thorough analysis using radio wave propagation theory is beyond the scope of the current paper, but will be part of future work. Moreover, we are not aware of similar ambiguous cases described in the scientific literature.

REVIEWER: *The manuscript is well structured, however, stylistics might be still improved, e.g. paragraphs in the result section could be more concise and fluent.*

RESPONSE: We will carefully re-read the manuscript and apply modifications where applicable.

REVIEWER:

Specific comments:

P7L28: Results and discussion section: The results of microwave links are in the text mostly presented in mm/h although figures show also dBs. I strongly recommend to present the results also in dBs and

compare them with theoretical rain induced attenuation from disdrometer data (eq. 3). The main reasons are these i) the uncertainties arising from imperfect separation of rain-induced attenuation are mixed with uncertainties arising from rainfall-attenuation powerlaw model, i.e. variability of α and β parameters (Tab. 2) during different rainfall events and uncertainties due to path-integration of attenuation and nonlinearity of power-law model. This hinders interpretation of results.

ii) Substantial part of link attenuation unexplained by raindrops are hardware related errors (e.g. due to wet antenna or quantization noise). Such uncertainties expressed in mm/h apply only to links of the same lengths as in the experiment.

iii) Most of the literature concerning microwave link propagation and different phenomena influencing radio wave attenuation (including wet antenna attenuation) express results in dBs.

RESPONSE: We completely agree with the reviewer on this point. We will add an extra panel to figures 5, 6, 8, 9, and 13, showing attenuation in dBs including the disdrometer-derived theoretical attenuations.

REVIEWER: *P8L5: It is stated here that in the presented event there are 'no attenuation-inducing influences other than rain', however, this is inexact as the radio waves are during this event for sure attenuated e.g. by atmospheric gases, there is a free space loss, etc.*

RESPONSE: This is meant as "no attenuating phenomena contributing to the dynamics of the signal". We will clarify this in the text.

REVIEWER: *P8L33: There are certainly various attenuating phenomena (see comment P8L5) influencing link attenuation, and drop down in the RAL link signal level has probably some (uknown?) reason.*

RESPONSE: We agree. We will alter the text on this point.

REVIEWER*: P9L4: 'remarkably stable' or 'uncertain baseline' is very subjective description. Please quantify.*

RESPONSE: Agreed. We will provide numbers in the revised version.

REVIEWER*: P9L17-20: The causes of outliers and overestimation discussed in these lines are speculative. The experimental design should enable investigate unexpected behavior of links much more specifically thanks to reliable ground truth, cameras, etc. For example, it is stated here that 'overestimation and outliers could be attributed to attenuating phenomena ... erroneously processed as rain in the basic algorithm'. It should be, however, possible to check against disdrometer data if the errors are due to the processing algorithm. Similarly, errors introduced by k-R model can be estimated and it should be verified if they can explain underestimation.*

RESPONSE: We have added to this response a new figure illustrating the relation between link attenuation and disdrometer-derived theoretical attenuation at the relevant frequencies. We also added an updated version of figure 7. These pictures show very similar results. Therefore, the R-k power law model introduces very little additional error. This is further supported by the high goodness-of-fit found for the R-k model itself. We will further clarify this in the text.

REVIEWER*: P10L22-24: Please quantify the magnitude of oscillations.*

RESPONSE: Agreed. We will quantify this magnitude.

REVIEWER*: P10L33: Is the 90 % humidity threshold selected arbitrary, based on radiowave propagation theories, or estimated by regression itself? Please indicate.*

RESPONSE: The reason for this is made clear in P11L8-11 when talking about dew. We will re-arrange the text so that this is clear when the 90% threshold is introduced.

REVIEWER*: P11L13-15: The statement that 'the temperature dependence of the Nokia link is drowned out in the noise' is speculative as you cannot prove there is a temperature dependency if it is*

'drowned out in the noise'. If you can prove it (at reasonable confidence level) it is then not 'drowned out in the noise'.

RESPONSE: We acknowledge that this phrasing is sloppy. We have rephrased: "There is no evidence of a temperature dependence of the Nokia link here, even though one would expect it based on the findings from 14-24 April."

REVIEWER: *P11L19: Please indicate in the text the duration of antenna wetting and drying quantitatively. The figures depict too long period to distinguish if the processes take place only few minutes, tens of minutes or few hours.*

RESPONSE: The timescale of these events is in the order of hours. We will add this information to the text.

REVIEWER: *P11L31-32: Please describe more precisely what is meant with 'quite different pattern'. Different range, variability, autocorrelation structure, ...?*

RESPONSE: We refer here to the autocorrelation structure. We will clarify this in the text and provide more detail.

REVIEWER: *P13L11-12: What is meant with 'any other atmospheric phenomena'? Furthermore, the following text relates the attenuation to the humidity which is an atmospheric phenomena. The whole meaning of this sentence is, therefore, unclear.*

RESPONSE: restated: "by any one atmospheric phenomenon as described in the previous sections"

REVIEWER: *P13L15-22: The antenna drying times might be very much influenced also by other environmental variables such as wind or sun radiation. Could e.g. wind which is also displayed in the figs 16 and 17 explain part of the uncertainty in drying duration? Is there any reason why humidity is included in the quantitative analyses and not the wind?*

RESPONSE: While an interesting topic, this would go beyond the scope of this paper. We will mention in the text that these phenoma could indeed influence the antenna drying times and that this is subject of future work.

REVIEWER: *P14L20: A robust evidence that the link response to the additive and multiplicative bias is consistent over different events has not been provided in the previous text. Why don't you e.g. quantify both additive and multiplicative bias for each event and link and provide information about range and variability of both types of biases?*

RESPONSE: Our statement refers to P9L5-14 and fig. 7. We feel that this provides enough evidence to make this statement. Computing these biases for each single event in the data set is beyond the scope of this paper.

REVIEWER: *Figures: There is a wrong legend in the panel (a) of the figures 5, 6, 8, 9, 10, 12, 15, 16 and 17 as RAL 38 V is assigned to both blue and green lines. It seems to be that green line belongs to the RAL 38 H and the orange one to the RAL 26 V, i.e. same coding as in the panel (b)*

RESPONSE: We thank the reviewer for catching this error! We will correct this.

Anonymous Referee #2

REVIEWER: *The authors have put together an experimental campaign in order to explore in depth some aspects of rainfall measurement from microwave links attenuation and understand better the uncertainties, focusing an a relatively short links (2 km) and medium high frequencies (26/38 GHz). The experimental set up is impressive and thorough, with 2 microwaves links –one operating at 38 Ghz and the other one dual frequency 38/26 GHz and dual polarization- sharing the same (2 km long) path ; 5*

disdrometers in order to analyze rainfall intensity and microphysical variability along the path and at both ends, and an additional rain gauge ; a near IR scintillometer, cameras and a met station complement the set up and provide additional information on visibility and other atmospheric variables that might influence or help understanding the MWlinks signal fluctuations.

This is an ideal setting to analyze and quantify – at least for the 2 frequencies and the path length that are available here – some of the uncertainties in MWlinks based Quantitative Precipitation Estimation : -variability and time/space scale issues in the k-R relationship -wet antenna attenuation -baseline derivation uncertainty and non-rain induced fluctuations of the signal

-Additionally the MWlink power level is sampled at 20 Hz and with a small quantization error - which could be used to investigate errors due to coarse quantization and to the subsampling of the signal typically provided by Commercial MWLinks network monitoring systems (only providing max and min power every 15 minutes is common).

-Also the dual-frequency and dual-pol capability, together with the 5 disdrometers will allow to go further than the simple k-R based retrieval.

First of all I would like to congratulate the authors for the experiment they have put together and acknowledge the amount of work and time which will be necessary to fully exploit such a data set !

RESPONSE: We thank the reviewer for the appreciation of our experiment and paper.

REVIEWER: *The main objective of the present paper is to present the experimental setting itself and some preliminary results which illustrate -in a rather qualitative manner- some of the issues that could be further explored with the data set : the discrepancy between the rainfall retrieved by the links and the path average rainfall retrieved by the 5 disdrometers, illustrated with 3 rainfall events ; some illustration of measurement during mixed precipitation ; effects of temperature on the signal fluctuations; wet antenna attenuation and its sensitivity to the type of radom material ; effect of dew and fog ; effect of clutter. Altogether an interesting catalog that illustrates the complexity of mwlink based retrieval of precipitation is provided in section 5. However, the reader stands a bit frustrated by a somehow QUALITATIVE OVERVIEW OF VARIOUS CAUSES OF MW SIGNAL FLUCTUATIONS, WITH A LACK OF STATISTICAL AND QUANTITATIVE ASSESSMENT OF THEIR IMPACT ON I) DETECTING/QUANTIFYING ATTENUATION DUE TO RAIN AND II) RETRIEVING RAIN RATE.*

RESPONSE: As the reviewer acknowledges, the point of this paper was to provide a somewhat qualitative overview of the issues which could be explored with this dataset. An in-depth analysis of any one of these issues would merit it's own separate treatment and is beyond the scope of this paper. We do intend to explore several of these issues further and we encourage others to do so as well once we have published the accompanying dataset. However, as we have also admitted in our response to referee #1, some of our statements in the results section are needlessly qualitative and could easily be made more quantitative. We will remedy this in a revised manuscript.

REVIEWER: *I would suggest that Sub-section 5.2, which has the most quantitative results and focus on the main objective of the MWlinks exploitation, i.e. rain retrieval, become a full section and be improved with some more quantitative results.*

The other sub-sections in 5 should be lightened (5.3 and Fig9 which is essentially qualitative can be suppressed) and more focused on explaining some of the discrepancies observed in 5.2.

RESPONSE: We believe that following the recommendation in this comment would not serve to improve the manuscript as it would radically alter the focus of the paper. We will hence keep the structure as it was. However, we will add more quantitative results wherever possible, as also indicated in our response to reviewer #1.

REVIEWER: *The text itself needs revising ; some expressions or comments are more subjective than scientific – and the authors sometimes overgeneralize their statements e.g. P4 L1 'the power law in the literature are ALL derived at point scale ' P 13 L12 'it is important to take into account that there will*

always be unexplained anomalies' P2 l 39 :' a relatively straightforward algorithm' P3 L31 'the relations ..... closely resemble power law' etc... see more below.

RESPONSE: We will revise the overgeneralized statements P4 L1 and P 13 L12. However, we do not believe that statements such as P2 L39 and P3 L31 are problematic. We will adapt the manuscript where applicable to make the wording less subjective.

REVIEWER: *DETAILed SUGGESTIONS : Title/Introduction :*

- The stress on urban in the title is misleading – the paper does not focus on an urban problem or urban hydromet scales specially. A tile like 'A multi-instrument microwave link measurement campaign' would be better. - The introduction also stresses a lot on urban scales which is not that relevant since a single link and not a dense network are studied here.

RESPONSE: The frequencies employed here are frequencies that are often used in operational networks in urban areas. Furthermore, although the experiment features a single link, the context for these research questions comes from the use of urban link networks. However, we acknowledge that the experiment itself is not necessarily only applicable to urban applications and we will adapt the title to reflect that.

REVIEWER: *- P1 L33-L35 confusion between the space/time resolution of a single gauge and the problem of gauge network density versus scale of phenomenon.*

RESPONSE: This text will be revised to make this distinction clearer.

REVIEWER: *- P2l8 : modern radar also used propagation variables such as Kdp and not just Z....*

RESPONSE: "radar" is now changed in the text to "traditional radar". Note that Kdp can only be used for rainfall estimation at high rain rates, so that even with dual-pol radar a relation between Z and R is needed for the lower rain rates.

REVIEWER: *-P2 L25 : 'therefore further research... ... microphysical aspects' – Sentence not clear + microphysics is not really the focus of this paper....*

RESPONSE: We will modify the text to read "Therefore, further research is needed regarding the physical aspects of the attenuation measurements themselves.".

REVIEWER: *- P2 L 27 : relevance of urban? ' in order to help fine tune the existing retrieval algorithm' - The sentence is clumsy and there is nothing about tuning the algorithm in the presented work anyway..... L 29: simulating links from radar data is not at all relevant to what is proposed here and to the local scale (one single 2 km path) studied.*

RESPONSE: P2L27-29 will be completely revised in the updated manuscript, and the sentence related to "simulated links" will be removed.

REVIEWER: *Section 2 – P3 L 29 ' the relations .... Resemble power laws' – Paragraph to be revised – false or approximative statements.*

RESPONSE: It is not clear to us what the referee means here. We see no false statements here. We will revise the wording of this paragraph to make it clearer.

REVIEWER: *k-R relationship discussion : the discussion on k-R is spread in different parts of the manuscript with no consistency . The paragraph starting on P3 L35 is rather confused. There seem to be a confusion between DSD/rain type variability between rainfall events and k-R variability as a function of the scale considered (point versus path...). The concept of 'control volum' is unexplained and unclear. P3 Eq(6) insists on the problem of linearity of the relationship and the problem of point versus path average k-R relationship - but the fact that in this work the path average k-R relationship is effectively derived thanks to 5 disdrometers in not mentioned. ...Subsection 4.1.2-4.1.3 should be merged and with a more explicit title like 'deriving path averaged k-R relationship'.*

RESPONSE: We do not use path-averaged rain rate and attenuation to derive an R-k relationship, but the point scale data from all disdrometers are employed. This would not make much of a difference anyway. The importance of the near-linearity of the R-k relationship is related to the variability of raindrop concentration and size distribution along the path and not directly to variability between different events or as a function of the scale considered. Using a path-averaged relationship would not solve the ambiguity unless one derives a new R-k relationship for every timestep for this particular path and rain field. This would defeat the point of doing a microwave retrieval in the first place! We admit that the phrasing used in P4L1 is misleading and we will revise it.

REVIEWER*: Also note that k=aR^b is used in (5 and 6) while a and b in Table 2 are for R=a k^b most confusing*

RESPONSE: Equation 5 and 6 are incorrect. Thank you for noting this. We will correct this.

REVIEWER: *Section 3 : P4 L25 – please give the same precision for the frequency of the Nokia and RAL links.*

RESPONSE: We will modify this.

REVIEWER: *L24 : 'representative of THE link systems that would be used ....' to be rephrased carefully – not all CMLs are Nokia and you dont use the NOKIA sampling/digitalization....*

RESPONSE: "representative" is changed in the text to "a typical example".

REVIEWER: *P4 L 31 : 'roughly' – unprecise L32-33 give the exact frequencies.*

RESPONSE: See our response above.

REVIEWER: *Section 4 4.1.2/4.1.3 – merge and improve. It seems that you are deriving a path-averaged k-R relationship based on weight values of both k and R derived from the 5 disdrometers with 30s long DSD spectra. Is this the case ? not very clear from the text. This very important point should stressed : most studies do not have access to the path average k-R and have to infer it from ponctual k-R and assumptions on rainfall variability . The differences between the single disdrometer and path averaged k-R should be discussed.*

RESPONSE: This is not the case and that fact is mentioned in the text : P6L40. We will add an extra clarification to P6L29.

REVIEWER: *P6L29-32 – earlier you mention that the disdrometer are evenly spread – so is this weighing really important ?*

RESPONSE: They are not evenly spread so this is important. This can be seen in Fig 1a. They were only as evenly spread as the limitations of the underlying terrain allowed (mainly access to large flat rooftops). This is maybe not clear from the phrasing in P5L14 so we will add a clarification here.

REVIEWER: *THE k-R (and not R-K otherwise do not use a and b as in (5 and 6)) relationships should be given here and the differences between previous studies and IUT discussed here and not introduced in conclusion. Also here is a good place to discuss point versus path k-R.... and your results on this with the 5 disdrometers.*

RESPONSE: We welcome this suggestion. We moved some of the discussion from section 6 to here.

REVIEWER: *P7 L 19 : the 24h centered window method is not applicable in RT (where you have access only to passed data - - and RT is mentioned in the introduction in the objectives of the work outcomes.....*

RESPONSE: We do not believe this is relevant. We never suggest that the methods used in this paper are directly applicable to operational settings.

REVIEWER: *Section 5 : P7 L 34 what is a 'relatively unambiguous event' ???*

RESPONSE: An event that can be related a single type of attenuating phenomenon, such as rain or dew formation on the antennas. In contrast to the compound phenomena in section 5.8. We will rephrase the text to make this clearer.

REVIEWER: *P7 L 35 : 'performance ... for detecting' : this is not done – there is no FAR/Miss study here – only analysis of the rainfall rate itself.*

RESPONSE: changed "detecting" to "measuring"

REVIEWER: *Section 5.2 : As mentioned, this could be enhanced and become the main result section. As suggested by reviewer 1 the analysis in terms of attenuation should be done first and then the retrieved Rain rates can be compared. One of the major surprise is the discrepancy between the two 38GHz/Hpol links rain retrieval, which is not fully explained by the paper and should be further explored in dB first. -what is the correlation and consistency between the time series of attenuation for the 2 links ? - the variability of the 2 signal in dry/wet periods should be further quantified (variance for instance).*

RESPONSE: As we mentioned above, making this section the main results section of this paper would greatly alter the focus of this paper, and we do not intend to do that. In our responses to reviewer #1, we have indicated that we will add comparisons in terms of specific attenuation. We have also indicated in our responses to reviewer #1 that we will quantify the signal fluctuations.

REVIEWER: *P8 – the analysis should be more objective and vocabulary such as 'visual inspection suggests' L35 ;' the magnitudes are similar' L15 ; 'loss seems almost entirely related to' L28 should be replaced by quantitative indicators.*

RESPONSE: We will revise these phrases.

REVIEWER: *P9 L1 : 'more spatially heterogeneous and probably convective' – please check and give some indicator of spatial heterogeneity – how is this affecting the path averaged versus punctual k-R on that day ?*

RESPONSE: Spatial heterogeneity can be indicated by the spatial coefficient of variation. We will add these numbers to the text. The high rainfall variability in time and space and the high rainfall rates are all indicative of convective rainfall. It has been shown (e.g. Berne and Uijlenhoet, GRL, 2007, Leijnse et al., JHM, 2010) that the effect of spatial variability on the k-R relation is limited at the frequencies under consideration.

REVIEWER: *P9 L17 to 25 : The discrepancies between links and between the link and disdro need to be further understood. What part can be explained by k-R variability ?; what comes from baseline error ? Comparison in DB first (with attenuations dervived from DSD spectra and your Tmatrix code) would help understanding.*

RESPONSE: See our response to comment P9L17-20 by reviewer #1.

REVIEWER: *Is a possible underestimation of rain rates by the DSD totally eliminated out ? What are the quantitative results of the gauge/DSD comparison for the 3 instruments that are gathered ?*

RESPONSE: This is beyond the scope of this paper.

REVIEWER: *The Conclusion will have to be adjusted when section 5 has been revised.*

RESPONSE: We will modify conclusions based on the modifications made in this paper. Note that the modifications that we will make are less than what reviewer #2 suggests. Hence the necessary modifications to the conclusions will be minor.

Anonymous Referee #3

REVIEWER: *Summary:*

This manuscript presents results from a comprehensive field experiment studying error sources for rainfall retrieval with microwave links. The paper is well structured and well written, expect for some places where the writing should be made less monotonous. The conclusion are a bit vague, though. However, in my opinion, this is more a shortcoming of the writing and less of the experimental setup or the analysis. In summary, this manuscripts provides an important contribution and should undergo a minor revision to be published in AMT.

RESPONSE: We thank the referee for the appreciative words. We will reformulate some of the vagueness in the text. See the specific comments for details.

REVIEWER: *General comment:*

The discussion of the causes, implications and possible mitigation strategies for the different effects should be more detailed in section 5. In particular the consequences when using data from a large number of operational microwave links from a cell phone network, where no ground truth is available to detect and accurately mitigate the caused errors, should be addressed. It would be important to, at least, estimate the magnitude of the different effects on rainfall retrieval from typical operational microwave link networks.

RESPONSE: Extension of the analysis to link networks is outside the scope of this work. However, we will provide a more thorough discussion of the causes, implications, and possible mitigation strategies for the different effects that we encounter in our data. This includes a discussion of the magnitude of the effects of the different phenomena.

REVIEWER: *The title and the abstract do not hold much information about the main goal and findings of this study, the search for explanations of the fluctuations of the received signal level. I recommend that the findings, which are a bit vague, but nevertheless very important for the community of researchers that derive rainfall information from microwave links, are presented clearer already in the abstract.*

RESPONSE: The Abstract will be adapted to include more of the findings.

REVIEWER*: Specific comments:*

Title: The title should reflect the actual topic, investigation of the microwave links errors, a bit more.

RESPONSE: The title will be replaced by one more appropriate to the contents of the paper.

REVIEWER*: page1, Line 18: With all the "and"s this sentence is a bit hard to understand*

RESPONSE: This sentence will be modified to improve its readability.

REVIEWER: *Page1, Line 25: Why not start a new paragraph here (instead of one sentence before) for the part of the abstract which summarizes the results.*

RESPONSE: We will implement this suggestion.

REVIEWER: *Page1, Line 27: I would not call "temperature" an "attenuating phenomena". As you show in the manuscript, it can have a big effect on the RSL, but not by adding attenuation. It is more likely to be bias from the electronics. Maybe you could reformulate here.*

RESPONSE: "attenuating phenomena" will be changed to "phenomena affecting received signal level".

REVIEWER: *Page1, Line 28: The summary of the conclusions should be more detailed. What is the order of magnitude of the different error sources, etc?*

RESPONSE: We agree with the reviewer that adding details about the magnitude of the effects of the different error sources will improve the paper. We will hence add general quantitative results.

REVIEWER: *Page 1, Line 36: Instead of "regional" precipitation distribution, writing "local" or just "spatial" fits better here.*

RESPONSE: Thank you for the suggestion. We will use "spatial".

REVIEWER: *Page 1, Line 38: Since the height of the radar observation above ground is very close to the ground near the radar, and can be a lot higher than 1000 meters far from the radar, I would not write "roughly 1000 meters" but maybe mention that it can be more than 1000 meters far from the radar or in complex terrain*

RESPONSE: We will change the text following the recommendation of the referee.

REVIEWER: *Page 2, Line 1: "arsenal" sounds a bit colloquial.*

RESPONSE: We will replace "arsenal" by "range"

REVIEWER: *Page 2, Line 10: Do you mean "back then" instead of "since then"*

RESPONSE: We do mean "since then", but we agree that the way it is used in this sentence is confusing. We will rewrite the sentence to become: "Despite these advantages, microwave links have not been deployed at a large scale for the purpose of precipitation monitoring, for the cost of setting up such a network would still have been quite severe.".

REVIEWER: *Page 2, Line 13: A bit monotonous: "This ... This ... This.."*

RESPONSE: We will some variation in the wording.

REVIEWER: *Page 2, Line 25: Add a comma after "Therefore ..."*

RESPONSE: We will add a comma.

REVIEWER: *Page 2, Line 25: Is "research ... into ... " correct english?*

RESPONSE: We will rewrite this to become: "Therefore, further research is needed regarding the physical aspects of the attenuation measurements themselves.".

REVIEWER: *Page 2, Line 25: When speaking about "microphysical aspects" of the "retrieval algorithm" I would think more towards the em-wave scattering of individual drops and not the error sources you are investigating here. Hence, I feel the term "microphysical" is misleading here.*

RESPONSE: See our response to the comment about this to reviewer #2. We will modify the text to read "Therefore, further research is needed regarding the physical aspects of the attenuation measurements themselves.".

REVIEWER: *Page 3, Line 31: Add comma after "on the other"*

RESPONSE: We will add a comma here.

REVIEWER: *Page 4, Line 24: Is the Nokia link working in both directions? If yes, what is the frequency difference?*

RESPONSE: The Nokia link is bidirectional, but only the received signal level at one end was recorded. The frequency of the reverse carrier wave is 39.436250 GHz.

REVIEWER: *Page 4, Line 32: Is the difference of only 176 MHz between the Nokia and the dual-pol RAL link really enough to make sure they do not interfere? To be more precise, do you know the band-pass filtering characteristics of both systems?*

RESPONSE: The bandwidth of the RAL receiver is 4 KHz, and the bandwidth of the Nokia receiver is 0.9 MHz. The bandwidth of the RAL transmitter is << 1 KHz and the bandwidth of the Nokia transmitter is 3.5 MHz. The difference of 176 MHz should therefore be enough to avoid interference. We will add additional information to the description of the links in section 3.2.

REVIEWER: *Question regarding the systems: Multipath effects can also cause large fluctuations in the received signal level. This effect will be different for different propagation settings, i.e. different*

frequencies and different antennas. What is the antenna size, beam width and gain for the used systems? Maybe a table with the details of the systems would be good.

RESPONSE: We will provide additional information on the antenna characteristics.

REVIEWER: *Page 4, Line 35: "This provides for comparison in the case of, ... ". Is the term, "to provide for comparison" correct English?*

RESPONSE: We believe it is. However, understand that the sentence may be difficult to read. We will alter this sentence to improve its readability: "This provides information about, for example, fog and other visibility-affecting phenomena.".

REVIEWER: *Page5, Line 7: Since you did not monitor the TX power, how about (temperature) drifts of the transmitter?*

RESPONSE: We do not make a distinction between temperature dependencies in the transmitter or the receiver.

REVIEWER: *Page 5, Line 11: Is "in this way" correct english?*

RESPONSE: We will modify this part of the sentence to become: "This information can be used to, for example, identify solid precipitation in the...".

REVIEWER: *Page 6, line 27: You use temperature observations for deriving the terminal velocity (as stated in section 4.1.1), but here you use a constant temperature of 15 degree Celsius. Why? In particular for 38 GHz, temperature difference e.g. between summer and winter, will impact the extinction cross section and hence the k-R relation.*

RESPONSE: This was done due to pragmatic reasons. However, the temperature dependence of the extinction cross section is very slight within the used temperature range and will not effect the R-K relation to a significant degree. See e.g. Olsen et al. (1978).

REVIEWER: *Page 7, Line 4: You should discuss how do the derived k-R parameters compare to the ones from the literature here.*

RESPONSE: We have moved the relevant parts of section 6 to section 4.1.3, so that this section now also includes a comparison with values from the literature.

REVIEWER: *Page 7, Line 6: It is a bit misleading that you write that you are "closely following" Overeem et al., but some sentences later write that you use a completely different way (which is fine for this experiment) to detect rain events.*

RESPONSE: This sentence is indeed misleading and an unfortunate remnant of earlier drafts. We will remove it.

REVIEWER: *Page 7, Line 13: "would not be relevant here", maybe better write "is not applicable here"*

RESPONSE: Agreed. We will rephrase this according to the reviewer's suggestion.

REVIEWER: *Page 8, Line 10: Are you sure this is "background noise", hence stemming from the electronics? It could also stem from propagation differences of the systems, e.g. because of different beam widths or slightly different alignments. Both of these could result in different propagation conditions resulting from diffraction/refraction from the ground (buildings, trees, etc.).*

RESPONSE: By using the term "background noise" we did not wish to imply that the source is with the electronics, but rather that the source is unknown and not related to the quantity of interest. Moreover, we are not talking about the "dry" received power level per se, but rather the variability within this power level for a single receiver as represented by the 5th and 95th percentile over the moving window. We will clarify what we mean by the "background noise level".

REVIEWER: *Page 9, Line 1: Add a "a" after "probably"*

RESPONSE: That does not seem right to us, as we have an "a" between "is" and "more".

REVIEWER: *General question: Doesn't the additive bias mainly stem from the very simple baseline determination?*

RESPONSE: Yes. We will expand upon this in the revised text.

REVIEWER: *General question: What is the correlation and bias of the disdrometer and the gauge next to it?*

RESPONSE: We will add this information to the manuscript.

REVIEWER: *Page 10, Line 4: The precipitation intensities should not only be "taken with a grain of salt". Their absolute values are, as you explain a little later, completely unusable. Maybe the dynamics indicate a little the dynamics of the precipitation event. But the problem most likely is that your 30-second disdrometer aggregations are too short and only contain a very small number of drops. Hence there is a lot of sharp isolated peaks which might probably stem from individual large snowflakes the disdrometer detected during on 30-second period.*

RESPONSE: We agree with the reviewer that the absolute values are incorrect. However, the dynamics of the intensity and the precipitation type are useful information, which is why we stated that they should be taken with ``a grain of salt´´. We will rephrase this subjective sentence to clarify this.

REVIEWER: *Page 10, line 16: Maybe, if available, you could add possible explanations for this effect if, as you write, the snow deposit alone cannot explain it.*

RESPONSE: One possible explanantion is antenna wetting due to the partial melting of the snow deposits on top of the antenna cover. However, at this point that is no more than speculation and we would need more research to confirm it.

REVIEWER: *Page 11, line 15: It is not clear from the text whether the periods with high humidity are also removed for the calculation of correlation including rainy periods.*

RESPONSE: We have not removed periods with high humidity for the computation of correlation coefficients in rain. We will clarify this in the text.

REVIEWER: *Page 11, line 15: "temperature dependence ... is still roughly consistent ...". First of all, the term "still roughly consistent" is a bit vague and should be rephrased. However, judging from table 1, there is a clear decrease of the correlation if rainy periods are included and a further decrease when only considering rainy period. I think, this should be reflected in the text. Nevertheless, the correlation of, e.g. -0.4 for rainy periods only, is surprisingly high.*

RESPONSE: We will revise the text accordingly.

REVIEWER: *Page 11, line 26: Does dew really build up a thin layer on the antenna or does it also form small droplets, as shown for the spraying of the antennas?*

RESPONSE: The effect is the same as for the artificial spraying. So, a nearly uniform layer on the Nokia and large drops on the RAL links. This can be observed in the time lapse camera footage.

REVIEWER: *Page 11, line 41: Fog cannot generate an attenuation of 3 dB for such short links at frequencies of 38 GHz and below (please check the references you cited). Hence, I do not understand why the you consider fog as a possible source in this sentence.*

RESPONSE: We agree with the reviewer that fog cannot generate an attenuation of 3dB for these links. However, part of the attenuation (up to 1.5 dB) can be caused by fog on the path, so this is why we do mention this here. We agree that the sentence can benefit from rewording to clarify what we mean: "However, both wetting of the antennas and the attenuation by the fog droplets themselves can

contribute to this attenuation, and it is difficult to estimate their respective relative contributions to the total attenuation.".

REVIEWER: *Page 13, line 19: "... no lingering attenuation, ..." This comma should be moved after "..in both cases ...".*

RESPONSE: We will move this comma.

REVIEWER: *Page 14, line 2: The comparison of the different parameters would fit better in section 4.1.3 where the actual analysis is explained. In the conclusion section I would not expect the presentation of new results or data.*

RESPONSE: This section will be moved.

REVIEWER: *Page 14, line 43: Will the data of the experiment be made available after publication?*

RESPONSE: Yes! We believe is is very important that others can also use this dataset. The raw data will be published as soon as we have made final quality control checks. In the mean time, the data will be available upon request from the corresponding author.

REVIEWER: *Fig 5: "RAL 38 V" appears two times in the legend. Colors of RAL 38H and RAL 26 change between plot "a" and "b"*

RESPONSE: This is unfortunate. The graphs will be fixed.

REVIEWER: *Fig 7: Why not use the same color for the different microwave links as in the time series plots, e.g. Fig 6.*

RESPONSE: This is a welcome suggestion. We will do so.

~~An urban~~A measurement campaign to assess sources of error in microwave link rainfall ~~measurement campaign~~estimation

Thomas C. van Leth[1], Aart Overeem[1,2], Hidde Leijnse[2], Remko Uijlenhoet[1]~~, Hidde Leijnse[2]~~

[1]Hydrology and Quantitative Water Management Group, Wageningen University, P.O. Box 47, 6700 AA, Wageningen, the Netherlands
[2]Royal Netherlands Meteorological Institute (KNMI), P.O. Box 201, 3730 AE, De Bilt, the Netherlands

Correspondence to: Thomas C. van Leth (tommy.vanleth@wur.nl)

Abstract. ~~Microwave links from cellular communication networks have been shown to be able to provide valuable information concerning the space-time variability of rainfall. In particular over urban areas, where network densities are generally high, they have the potential to complement existing dedicated infrastructure to measure rainfall (gauges, radars). In addition, microwave links provide a great opportunity for ground-based rainfall measurement for those land surface areas of the world where gauges and radars are generally lacking. Such information is not only crucial for water management and agriculture, but also for instance for ground validation of space borne rainfall estimates such as those provided by the GPM (Global Precipitation Measurement) mission.~~

~~The campaign described in this paper is dedicated to address several errors and uncertainties associated with such quantitative precipitation estimates in detail.~~ We present a measurement campaign to address several error sources associated with rainfall estimates from microwave links in cellular communication networks. The core of the experiment is provided by three co-located microwave links installed between two major buildings on opposite sides of the small town of Wageningen ~~University campus~~, approximately 2 km apart: a 38 ~~-~~GHz formerly commercial microwave link, ~~and~~as well as 26 GHz and 38 GHz (dual-polarization) research microwave links. Transmitting and receiving antennas have been attached to masts installed on the roofs of the two buildings, about 30 m above the ground. This setup has been complemented with an infrared large-aperture ~~Scintillometer~~scintillometer, installed over the same path, as well as 5 laser disdrometers ~~and an automated rain gauge~~ positioned at several locations along the path~~.~~ and an automated rain gauge. Temporal sampling of the received signals was performed at a rate of 20 Hz. The setup ~~is being~~was monitored by time-lapse cameras to assess the state of the antennas as well as the atmosphere. The experiment has been active between August 2014 and December 2015.

Data from an existing automated weather station situated just outside Wageningen was further used to compare and to interpret the findings. ~~We find that a basic rainfall retrieval algorithm with no corrections already provides a reasonable correlation to rainfall as measured by the disdrometers. The microwave links do give a significant overestimation. We further investigate~~In addition to presenting the experiment, we also conduct a preliminary global analysis and show several ~~events covering~~cases highlighting the different ~~attenuating~~ phenomena affecting received signal levels: Rainfall, solid precipitation, temperature, ~~dew~~ fog, antenna wetting due to rain or dew, and clutter. We also briefly explore cases where several phenomena play a role. ~~We conclude that the~~A rainfall intensity (R) – specific attenuation (k) relationship was derived from the disdrometer data. We find that a basic rainfall retrieval algorithm without corrections already provides a reasonable correlation to rainfall as measured by the disdrometers. However, there are strong systematic overestimations (factors of 1.2–2.1) which cannot be attributed to the R–k relationship. We observe attenuations in the order of 3 dB due to antenna wetting under fog or dew conditions. We also observe fluctuations of a similar magnitude related to changes in temperature. The response of different makes of microwave antennas to many of these phenomena is significantly different even under the exact same operating conditions and ~~configuration~~configurations.

1 Introduction

Accurate and real-time precipitation measurements are important for flood prediction, especially in urban areas. Traditional measurement techniques such as rain gauges have an insufficient temporal and spatial ~~resolution~~network density to allow for accurate measurements in an urban setting (Berne, et al., 2004; Schilling, 1991). Furthermore, their spatial representativeness is limited because of their small sampling areas, making them essentially zero-dimensional point measurements. Weather radars, in contrast, have a much larger sampling area and provide full coverage making ~~them~~their observations more representative of the ~~regional~~spatial precipitation distribution, but their space-time resolution is often limited, in particular for urban applications. Furthermore, ~~since they measure high~~radar observations take place higher up in the atmosphere ~~(roughly~~the further away they are from the radar antenna (typical observation heights can be more than 1000 ~~meters),~~m). Therefore, their measurements may not be representative of the situation near ground level. Finally, their high cost may be prohibitive for use by developing countries or local authorities.

Microwave link measurements may be a promising addition to the existing ~~arsenal~~range of rain measurement techniques. The use of such instruments for measuring ~~precipitation~~rainfall was first suggested by Atlas and Ulbrich (1977). With respect to spatial representativeness and resolution, microwave links can fill some of the gaps between rain gauges and weather radar. The area sampled is along the path of the link: typically about a few kilometers long and a few meters to tens of meters wide at the widest point. This makes the sampling footprint approximately one-dimensional. This is more spatially representative than a rain gauge, but less so than radar. However, microwave links have two major advantages over radar: they measure much closer to the ground than radar (typically a few tens of meters), and the relation between the measured variable (specific attenuation in the case of links and radar reflectivity in the case of traditional radar) and rainfall intensity is much better defined and closer to linear for microwave links.

Despite these advantages, microwave links had not been deployed at a large scale ~~since then~~for the purpose of rainfall monitoring, for the cost of setting up such a network would still have been quite severe. The real potential of microwave link measurements for ~~precipitation~~rainfall measurement came with the realization that the microwave links used in cellular communications networks could be repurposed as ~~precipitation~~rainfall measurement devices~~. This~~, which was demonstrated by Messer et al. (2006) and Leijnse et al. (2007a). ~~This~~Doing so eliminates most of the cost of this technique as existing infrastructure can be used. This is especially valuable in developing countries, which typically have few rain gauges let alone weather radar, yet do often have an extensive cellphone network (Doumounia, et al., 2014).

In the recent past there have been a number of studies towards the application of commercial microwave link networks for precipitation measurements. These studies have demonstrated the feasibility of this method in Southern Germany (Chwala, et al., 2012), the Netherlands (Overeem, et al., 2011; 2013), Israel (Zinevich, et al., 2008; 2009) and also in Burkina Faso (Doumounia, et al., 2014) and Brazil (Rios Gaona, et al., 2017).

Although the rainfall maps produced by this method show surprisingly good correspondence with the gauge-adjusted radar product (Overeem, et al., 2013), there are still inaccuracies remaining in the final products (Leijnse, et al., 2008; 2010; Zinevich, et al., 2010). Error sources can generally be divided into errors due to the mapping of the rainfall estimates from the microwave links, and errors in the individual measurements and the rainfall retrieval algorithm. It is in this last category where the largest remaining sources of error reside and not in the mapping (Rios Gaona, et al., 2015). Therefore, further research is needed ~~into~~regarding the ~~microphysical~~physical aspects of the ~~retrieval algorithm.~~

~~We present preliminary results from an experiment with three microwave links intended to investigate several possible sources of error in an urban environment in order to help fine-tune the existing retrieval scheme as laid forth in Overeem et al. (2011) and Overeem et al. (2016a) without resorting to simulated links from radar data.~~attenuation measurements themselves. Several possible sources of error affecting the quality of rainfall retrievals from single microwave links have been identified previously: the wet antenna effect and related dew formation on antennas (Minda & Nakamura, 2005; Leijnse, et al., 2008), humidity (Holt, et al., 2003) and temperature (Minda & Nakamura, 2005), solid precipitation and spatial variability of

precipitation (Berne & Uijlenhoet, 2007). Opportunities for simultaneous measurement of other environmental variables than rainfall have also been identified, such as evaporation (Leijnse, et al., 2007b), fog (Liebe, et al., 1989; David, et al., 2013), humidity (Chwala, et al., 2014) and hydrometeor type (Cherkassky, et al., 2014).

In this paper we describe a dedicated microwave link experiment that has been set up in the college town of Wageningen and ~~analyze~~present an analysis of the results. The field experiment has been designed to provide validation data for microwave link rainfall retrieval at the scale of a single link, and to be able to compare different types of links simultaneously measuring along the same path. The goal of the analysis is to give a comprehensive overview of the phenomena encountered by a typical microwave link and to evaluate their relevance to a rainfall intensity retrieval. In order to do so we employ a relatively straightforward retrieval algorithm with a minimum number of corrections and make use of a number of auxiliary measurement devices to gain insight into the retrieved signal. In ~~section~~Sect. 2 a brief overview of the theoretical background pertaining to the operating principles of microwave link rainfall measurements is given. Section 3 covers a description of the experimental setup and the employed instruments. In ~~section~~Sect. 4 the data processing methods applied in this experiment are detailed. In ~~section~~Sect. 5 the obtained experimental data is presented and an inventory of encountered phenomena is given. Finally, in ~~section~~Sect. 6 conclusions are drawn.

2 Theoretical background

Both the attenuation of a microwave signal by rain drops during a rain event and the corresponding ~~precipitation~~rainfall intensity can be related to the rain drop size distribution. The ~~precipitation~~rainfall intensity (in mm h^{-1}) can be calculated as follows, assuming the density of water to be constant:

$$R(t) = C_R \int_0^\infty V(D) v(D) N(D,t)\, dD \quad (1)$$

~~Where~~Here $V(D)$ is the volume of a raindrop in mm^3, D is the raindrop diameter in mm, $v(D)$ is the fall velocity (in m s^{-1}) of a particle with diameter D and $N(D,t)$ is the density of particles with diameter D per m^3 or drop size distribution (DSD) as a function of time t and $R_C = 3.6 \cdot 10^{-3}$ is a unit conversion factor. When dividing the particle diameter into discrete classes (as is measured by a disdrometer) this can be approximated as follows:

$$R(t) = C_R \frac{1}{6}\pi \int_0^\infty D^3 v(D) N(D,t)\, dD \approx C_R \frac{1}{6}\pi \sum_{i=1}^{n} D_i^3 v(D_i) N(D_i,t) \Delta D_i \quad (2)$$

Here, D_i is the mean diameter of the i_{th} drop size class, $N(D_i,t)$ is the discrete drop size distribution. ΔD_i is the width of the i_{th} diameter class, and n is the number of drop size classes.

A similar function defines the specific (logarithmic) attenuation (in dB km^{-1}), where we assume that the particle density is low enough such that multiple scattering can be neglected:

$$k(t) = C_{\sout{k}k} \int_0^\infty \sigma_{ext}(D) N(D,t)\, dD \approx C_k \sum_{i=1}^{n} \sigma_{ext}(D_i) N(D_i,t) \Delta D_i \quad (3)$$

Here, $\sigma_{ext}(D)$ (in mm^2) is the extinction cross-section of a hydrometeor with a diameter D and $C_k = 100 \cdot \ln(10)^{-1}$ is a unit conversion factor. $\sigma_{ext}(D)$ is also dependent on the frequency and polarization of the incident radiation. It can be derived from the forward scattering amplitude matrix $\boldsymbol{S}(D)$ which relates the incoming electromagnetic wave with the outgoing (forward scattered) wave~~:~~.

$$\begin{pmatrix} E_h \\ E_v \end{pmatrix} = \boldsymbol{S}(D) \begin{pmatrix} E_{h0} \\ E_{v0} \end{pmatrix} = \begin{pmatrix} S_{hh}(D) & S_{hv}(D) \\ S_{vh}(D) & S_{vv}(D) \end{pmatrix} \begin{pmatrix} E_{h0} \\ E_{v0} \end{pmatrix} \quad (4a)$$

$$\begin{pmatrix} \sigma_{ext,h}(D) \\ \sigma_{ext,v}(D) \end{pmatrix} = \frac{\lambda^2}{\pi} \Im \left[\begin{pmatrix} S_{hh}(D) \\ S_{vv}(D) \end{pmatrix} \right] \quad (4b)$$

~~Where~~where λ is the wavelength of the radiation in mm, S_{ij} is the element of the scattering amplitude matrix for the component of radiation with incoming polarization i and outgoing polarization j, where v and h represent the vertically polarized and horizontally polarized components, respectively (van der Hulst, 1957). The forward scattering amplitude matrix for spheres of arbitrary size and dielectric properties can be calculated with Mie scattering theory (Mie, 1908). In order to be

able to calculate the scattering properties for non-spherical drop shapes, we make use of the T-matrix approach (Waterman, 1965; Mishchenko, et al., 1996).

The relations between the raindrop diameter on the one hand, and the raindrop fall speed~~,~~ and its extinction cross-section ~~(and the differential phase)~~ on the other, closely resemble power laws (e.g. Atlas and Ulbrich, 1977). This means that both the specific attenuation and the precipitation intensity are approximately statistical moments of the DSD, which can themselves be empirically related by a power-law~~:~~.

~~$k = aR^b$~~ $k R = a k^b$, (5)

~~Where a and b are fitted parameters (Atlas & Ulbrich, 1977) which are both dependent on the average DSD within the control volume.~~

~~The power law parameters derived for a small control volume are strictly speaking only valid for a larger volume when the rainfall intensity within that control volume is homogeneous. (Similar considerations apply for temporal aggregation.) When measuring path integrated attenuation with path lengths typical for a cellular communication link, this is no longer the case. Because the power law relationships employed throughout the literature are all derived at the point scale (including this paper) the validity of those relationships at the path scale is therefore dependent on the near linearity of Eq. (5) (that is: $b \approx 1$) at the relevant carrier frequencies, such that:~~

~~$A = \int_0^L k(s)\,ds = \int_0^L aR(s)^b\,ds \approx aL\langle R\rangle^b$~~ (6) where a and b are fitted parameters (Atlas & Ulbrich, 1977) which are both dependent on the average DSD as well as the temporal and spatial distribution of the DSD within the measured volume. Because of the dependency on these DSD characteristics, power-law parameters derived from a particular set of observations would strictly speaking only be valid for links that have the exact temporal and spatial distribution of drop sizes and concentrations within their path. This would mean that, even under the assumption of a uniform and unchanging DSD for a given climate, rainfall variability and intermittency within the link path volume as a rain event evolves or passes over would lead to inaccurate estimation of R with this method. However, at the carrier wave frequencies typically employed in cellular communications links, the integrands in Eq. 1 and Eq, 2 are of a similar magnitude; As a result the R–k relationship is almost independent of the DSD and the exponent b is close to 1 (Olsen et al, 1978; Leijnse et al., 2007c). Therefore, an R–k relationship derived for this range of frequencies could be valid for a broad range of events. Furthermore, because of the near-linearity of the relationship, parameters derived from either point measurements of the DSD or path-averages of the DSD can be used to derive path-average rainfall intensities from path-integrated attenuation in heterogeneous rain fields:

$\langle R\rangle = \frac{1}{L}\int_0^L a\,k(s)^b\,ds \approx \frac{1}{L}a[\int_0^L k(s)\,ds]^b = \frac{1}{L}a\,A^b$ (6)

Here L is the length of the link path, $k(s)$ is the specific attenuation at position s and A is the path-integrated attenuation.

3 Experimental setup

3.1 Global overview

The backbone of the experimental setup consists of three microwave links placed along the same path between two university buildings on opposite sides of the college town of Wageningen. As such, the majority of the 2.2–km long link path covers urban terrain (Fig. 1a). All transmitting antennas are placed on a ~~two meter~~2 m high mast at approximately 1.5 ~~meter~~m from the base of the mast (Fig. 1b). The mast is placed on top of a 7-story building. The building is situated atop a slightly elevated area on the south end of Wageningen (51.968657 °N, 5.68273 °E). The receiving antennas are placed on an identical mast on the roof of an 8-story building at the northern end of Wageningen (51.985230 °N, 5.664312 °E). The height above ground level is 27 ~~meter~~m on the transmitting end and 40 ~~meter~~m on the receiving end. The total height above sea level is 62 ~~meter~~m

at the transmitting end and 51 ~~meter~~m at the receiving end. The terrain in between the endpoints of the path consists mostly of terraced housing, a sports field and other buildings of three stories or less. The maximum width of the first Fresnel zone (halfway along the path) at the featured frequencies is less than 5 ~~meter thus~~m. Thus, considering the height of the antenna locations compared to the intermediate terrain, there are no permanent obstructions affecting the beam significantly.

The experiment has been operational from 22 August 2014 up to and including 8 January 2016. Not all instruments have been operational during this entire period though, as is indicated in Fig. 2. Also, from 7 August 2015 to 25 August 2015 all transmitters were nonoperational due to a local power outage.

3.2 Microwave and near-infrared links

Of the three links one is a Nokia Flexihopper~~,~~ (Nokia), formerly part of a commercial cellphone network operated by T-Mobile. Such links are still used in cellphone networks around the world and this microwave link could therefore be regarded as ~~representative~~a typical example of the link systems that would be used in an operational setting. The Nokia ~~Flexihopper~~is a bidirectional link, but only one receiver was logged in this experiment. It is set to transmit and receive at a frequency of 38.17625 GHz in one way (which was recorded) and 39.43625 GHz in the other. The bandwidth of the signals is 0.9 MHz. The device transmits and receives only horizontally polarized radiation.

The other two links are custom-built by Rutherford Appleton Laboratories (UK) (RAL). The first operates at 26.00000 GHz and transmits and receives only horizontally polarized radiation. It contains both a linear and a logarithmic detector. The second RAL link operates at 38 ~~GHz.~~.00000 GHz. The bandwidth of the receivers is 4 KHz, while the transmitted signal bandwidth is extremely narrow (<< 1 KHz). Their oscillators are locked to GPS and therefore extremely stable. The receiver contains four detectors, two of which measure horizontally polarized radiation (linear and logarithmic) and the other measures vertically polarized radiation (idem). The phase difference between the horizontally and vertically polarized signals is measured by separate detectors as well. In this paper we will only deal with data from the logarithmic detectors. Note that the second RAL link measured at roughly the same frequency as the Nokia link. The frequencies are chosen to be far enough apart so as not to cause interference, but are close enough that the scattering characteristics of the radiation with respect to raindrops are almost identical. Additional characteristics of the link antennas are given in Table 1~~Table 1~~.

A Scintec BLS900 near-infrared ~~link~~boundary layer scintillometer is also placed together with the microwave links on the same path. It operates at a frequency of 340 THz (880 nm). This provides ~~for comparison in the case of~~information about, for example, fog and other visibility-affecting phenomena. Similarly to the microwave links (despite operating in a different scattering regime), it could potentially also be used to ~~measure~~estimate rain intensity (Uijlenhoet, et al., 2011).

All link receivers are sampled with a Campbell Scientific CR1000 data logger and stored on a remote server on a daily basis. The sampling frequency is 20 Hz. Auxiliary data (e.g. operating temperature) is sampled at a frequency of 2 min^{-1}. The Nokia ~~Flexihopper~~ system consists of separate outdoor and indoor units, the latter containing the digital signal processing circuits and power supply. Note that we have not actively used the indoor unit of the Nokia link system aside from the power supply; Instead, the analog detector signal normally used for ~~automated~~automatic gain control (AGC) is fed directly into the analog-digital converter (ADC) of the separate data logger. We do this to avoid the significant power quantization error (1 dB) that would be incurred using the link device's own AGC-ADC system. The analog signal was calibrated in an indoor environment using the signal power indication of the indoor unit as a reference. The RAL links ~~where~~were recalibrated by Rutherford Appleton Laboratories shortly before the beginning of the experiment. The calibration curves are shown below in Fig. 3. The transmitted power for all devices was kept constant, but was not separately measured.

3.3 Additional instruments

To serve as a ground truth, we use OTT Parsivel laser disdrometers (Fig. 1c). These can measure not only precipitation intensity but also the size and velocity distributions of passing precipitation particles over 30-s intervals. With this information they can

provide an approximation of the type of precipitation that occurred. In this ~~way~~manner it is possible to, for example, filter out solid precipitation from the microwave link data or select dry periods to determine the 'dry' baseline signal. Because of the small sampling footprint of these devices, they may not give a representative ground truth for the aggregated path measurements. Therefore five disdrometers are placed at four different locations, ~~roughly evenly~~ spread along the link path (Fig. ~~1a).~~1a) as evenly as was possible given the urban terrain. At the receiver end of the link path two disdrometers are placed next to each other in close proximity in order to test the accuracy of the disdrometers themselves. All disdrometers are placed on flat or gently sloping rooftops within Wageningen. The disdrometers all contain a built-in preprocessing unit which samples the raw laser amplitude signals, converts them to hydrometeor counts using an algorithm (undisclosed by OTT) based on the principle described in Löffler-Mang & Joss (2000) and aggregates the samples to 30-second intervals. One of the disdrometers at the receiver end has been operational since the beginning of the experiment. It is connected to the same data logger as the link detectors. The other four disdrometers have been operational for a shorter timespan (see Fig. 2). They are each connected to a UMTS modem which relays the disdrometer data to a remote server in real time. See Jaffrain et al. (2011) for more details about these autonomous disdrometer stations.

At the receiver end of the link path an automated tipping bucket rain gauge is placed close to the two disdrometers (Fig. 1d), to provide an additional independent measurement. The gauge has a tipping volume of 0.1 mm. Two time-lapse cameras are placed at each end of the link path. On each side one camera is pointed along the path and the other is pointed at the antennas themselves. These serve to allow visual inspection of the link path and the antennas, which can be useful for relating link behavior to physical events~~..~~.

For the subsequent data processing we also make use of data from the nearby ~~automated~~automatic weather station "Veenkampen" situated roughly 2 km to the west of Wageningen (operated by the university's Meteorology and Air Quality group) for ambient temperature and pressure measurements.

4 Data processing

4.1 Disdrometers

4.1.1 Preprocessing

The raindrop size and velocity distributions are corrected for known instrumental biases using the method of Raupach and Berne (2015), which involves two steps. Step one is shifting the velocity distributions so that the average velocities per size class match the theoretical terminal velocities for raindrops of that size class. Step two is multiplying the number of detected particles per size class by a class- and rain intensity-dependent correction factor. These correction factors were obtained by Raupach et al. (2015) from concurrent measurements with a 2D video disdrometer (2DVD), assuming the 2DVD measurements to be unbiased. Using these corrected distributions we derive rain intensities and other bulk quantities.
Whereas Raupach et al. (2015) use the theoretical raindrop terminal velocity model of Beard (1977) to determine the bias in velocity distribution we use the model of Beard (1976). The former is a simplification and approximation of the latter, designed to reduce computational expense. However, we found that on a contemporary desktop computer the time needed to compute terminal velocities was negligible using either model. Both models need the ambient pressure and temperature to calculate the raindrop terminal velocity. We used the temperature and pressure measured by the ~~automated~~automatic weather station "Veenkampen". Because this station is situated outside the built-up area of Wageningen, there might be a slight bias in temperature as compared to the urban areas that the disdrometers are situated in.

The model of Beard (1976) does not compute the terminal velocity directly from only the pressure and temperature but instead needs the density of the water drops and ambient air as well as the surface tension of the air-water interface as input. For the density of water as a function of temperature we use the empirical formula of Kell (Battan, 1973). For the surface tension of the air-water interface we employ the empirical relation proposed by Vargaftik et al. (1983).

4.1.2 Derived data

In the subsequent analysis we compare the attenuation encountered by the microwave link signals with the ~~precipitation~~rainfall along the link path. We also make use of a R–k ~~-R~~ relationship based on the actual ~~precipitation~~rainfall along the path and the expected attenuation due to this ~~precipitation~~rainfall. In order to do so, we assume that the corrected drop size distributions obtained from the disdrometer stations represent the ground truth for that location. The specific attenuation is derived from the drop size distributions using Eq. (3) and Eq. (4). We derive values for a carrier frequency of both 38 GHz and 26 GHz and for both horizontally and vertically polarized radiation.

We calculate the scattering amplitude matrix for each diameter class using the T-matrix approach developed by Waterman (1965). The computations are done using an algorithm adapted from FORTRAN code developed by Mishchenko et al. (1996; 1998; 2000) and reimplemented using the Python programming language. Since the laser disdrometer cannot provide information on the geometric shape or orientation of the particles, we make use of an orientation averaging scheme. For this purpose we have adapted the particle orientation averaging functions developed by Leinonen (2014) from their T-matrix package. The shape of the raindrops is approximated by an oblate spheroid, with axis ratio dependent on the volume-equivalent diameter. We use the axis- ratios suggested by Thurai et al. (2007). The complex index of refraction is needed to calculate the T-matrix. For rain drops we assume the empirically determined formula for the temperature-dependent complex index of refraction for pure liquid water by Liebe et al., (1991) where we use a temperature of 15 °C. ~~Precipitation~~Rainfall intensity is calculated with Eq. (2), using the corrected drop size distributions.

All derived disdrometer quantities are then averaged over the link path using a weighted average over all five disdrometers~~.~~, for the purpose of providing a comparison for the link measurements. For each point along the path, the value of the quantity is taken to be equal to the value derived at the nearest disdrometer. The mean over the path is therefore equal to the mean of the disdrometers weighted by the fraction of the path that is closest to that disdrometer. The precipitation type and presence as determined by the Parsivel algorithm are also used. In this case, the path-averaged type is assigned as 'mixed' whenever two or more Parsivels register different precipitation types. It is considered 'dry' only when all Parsivels agree that there is no precipitation. In all other cases when one or more Parsivels detect precipitation, that precipitation type is assigned as the path-averaged value. We distinguish five broad categories of precipitation: liquid, snow, hail/ice pellets, graupel, and mixed/melting snow. In the subsequent analyses we will mostly be concerned with liquid precipitation, since the other types ~~where~~were rare during the observation period.

4.1.3 ~~Attenuation-rainfall~~Rainfall intensity – specific attenuation relationship

The disdrometer-derived ~~precipitation~~rainfall intensities and specific attenuations at the frequencies employed in the microwave links are plotted with respect to each other in Fig. 4. Each dot represents a single 30-s ~~disdrometer~~DSD measurement (not path-averaged~~).~~) from an individual disdrometer. Measurements from all five disdrometers were used. Only data points that were characterized as liquid precipitation by the Parsivel algorithm and where ~~precipitation~~rainfall intensity was higher than 0.1 mm h^{-1} ~~where~~were selected. These data were then used to fit ~~a~~R–k power-law ~~model~~models using a non-linear least-squares algorithm. Goodness-of-fit for these relationships is very high: $R^2 = 0.956$ to $R^2 = 0.986$. Also note that the power-law exponents are all close to one, indicating that specific attenuation and rainfall intensity are nearly proportional to each other at the employed frequencies. These relationships can then be applied to the specific attenuations measured with the links.

In Table 2, the determined parameters are compared with others found in the literature. The parameters found by Leijnse et al. (2010) were based on drop size distributions collected in the Netherlands as well, but were collected using filter-paper in 1968 (Wessels, 1972). We also compare with the formal ITU (International Telecommunications Union) recommendation regarding the modelling of microwave attenuation due to rain (ITU-R Recommendation, 2005). We see that the exponents (b) are very similar for the relationships obtained in this work and those obtained by Leijnse et al. (2010) and

the coefficients (a) found by Leijnse et al. (2010) are somewhat lower than those found here. We can also conclude that the a parameter is too low and the b parameter is too high in the ITU recommendation for the Dutch rainfall climatology. For the analyses in Sect. 5 we have used these locally-derived power laws where applicable.

4.2 Microwave links

~~The microwave link received signal levels were converted to rain intensities using a baseline algorithm closely following the algorithm used by Overeem (2011; 2013).~~

In order to calculate the rainfall intensities, the attenuation caused by ~~precipitation~~rainfall and the attenuation caused by other atmospheric effects must be distinguished. Rahimi et al. (2003) proposed a two-step approach in order to do so.

The first step is to determine which of the sampled periods are dry. Overeem et al. (2013) ~~used~~uses the assumption of spatial correlation of ~~precipitation~~rainfall to determine 'wet' and 'dry' periods for microwave links in cellular communication networks. In short, a period is considered 'wet' if nearby links show a mutual decrease in received signal levels. As we are considering only a single path, such a method would not be ~~relevant~~applicable here. An alternative is to use the assumption of temporal correlation of ~~precipitation~~rainfall. Schleiss et al. (2010) suggested using a moving window standard deviation threshold. Similarly, Chwala et al. (2012) used a Fourier-transform based method to distinguish between wet and dry spells. Other methods applicable to a single link path are e.g. a Markov switching algorithm (Wang, et al., 2012) and the use of dual-frequency links (Rahimi, et al., 2003). Here, the path-aggregated disdrometer data is used to determine dry periods independently of the microwave link data.

The second step in the algorithm is to determine a suitable baseline signal level using the selected dry periods. The implemented baseline algorithm uses a rolling median over all measurements classified as dry in the surrounding centered 24-hour period to determine the baseline signal for each time~~-~~ step. The specific attenuation is then calculated as~~:~~

$$k = \max\left(\frac{Rx_{ref} - Rx}{L}, 0\right) \quad (7)$$

~~Where~~where Rx is the received power and L is the path length. ~~Precipitation~~Rainfall intensity is derived from the corrected attenuation using the power-law relationship of Eq. (5). The parameters a and b in this equation are obtained from the disdrometer data as described in ~~section~~Sect. 4.1.3.

The ~~precipitation~~rainfall intensity is furthermore set to 0 when the disdrometer indicates dry weather. Note that we do not perform any a priori additional corrections on the microwave link ~~precipitation~~rainfall estimate, such as correcting for wet ~~antennas~~antenna attenuations. The goal is, after all, to use this basic estimate to assess potential error inducing phenomena, not to evaluate a best~~-~~effort estimation.

5 Results and discussion

5.1 Overview

In the following section, we use the rainfall intensity as measured by the Parsivel disdrometers as a reference to assess the link-derived ~~precipitation.~~rainfall. Unless stated otherwise, we use the corrected DSD-derived rainfall intensities, not the rain intensities that the internal Parsivel algorithm produces.

In order to better understand the different phenomena that contribute to the microwave link attenuation signal, we present a number of illustrative events from the dataset. We search for ~~relatively unambiguous~~ events that can be related to a single type of attenuating phenomenon in order to gain insight into the separate phenomena. We will first ~~look at~~analyse the performance of the simple algorithm for ~~detecting~~measuring liquid precipitation and take a quick look at solid precipitation. We will then show how temperature and dew formation at the antennas affect the signal. ~~At the end~~Finally, we will look at some currently unexplained phenomena and also give some examples where different phenomena occur simultaneously.

5.2 Rainfall events

We compare the link-derived rainfall rates using the simple algorithm (excluding any specific corrections) described in ~~section 4.2 with the spatially averaged rainfall rates derived from the disdrometers using the corrected DSDs.~~ Sect. 4.2 with the spatially averaged rainfall rates derived from the disdrometers using the corrected DSDs. As a measure of the fitness of the disdrometer measurements as a ground truth, we first compare the collocated disdrometers with the tipping bucket rain gauge and each other. We used data of the entire measurement period where rain intensities higher than 0.1 mm h^{-1} were registered. We find that the correlations of the disdrometers with the rain gauge ($r = 0.928$ and $r = 0.927$) were only slightly lower than the correlation of the disdrometers with each other ($r = 0.959$). The mean differences between the disdrometers and the rain gauge were 0.039 mm h^{-1} and 0.129 mm h^{-1}, respectively, while the mean difference between both disdrometers amounted to 0.074 mm h^{-1}. That means that the disdrometers slightly overestimate the rain intensities as compared to the rain gauge, but this is of the same order of magnitude as the differences between the identical collocated disdrometers. Therefore, we will assume the path-averaged disdrometer measurements to be the 'true' path-averaged rainfall for the purpose of evaluating the link measurements.

Figure 5 shows an example of a single short isolated rain event on 14 July 2015 as indicated by the disdrometers. We chose this example because there are no ~~attenuation inducing influences~~ attenuating phenomena contributing to the dynamics of the signal other than rain in this event. ~~(~~Note that the received signal level of the Nokia ~~Flexihopper~~ is offset by 14 dB in order to fit into the plot. This is done consistently for all following figures~~)~~. Because the received power level can vary within the dry periods which we use to determine the baseline power level, we also indicate the 95th and 5th percentile of the received power level over the dry intervals within the surrounding 24-hour moving window. This gives an indication of the range of values that the power level might have had if there was no rain. Thus, if the rain-induced attenuation is within this range, it could not have been resolved from magnitude alone. The event consists of two distinct small peaks. The first peak of the path-average rainfall intensity only reaches 0.7 mm h^{-1}, while the second peak reaches 8 mm h^{-1}. We see that the second peak causes a clear attenuation of the received signal level of all the links. The smaller peak in rain intensity causes only a small attenuation in the 38 GHz links, fully within the 95th and 5th percentile range of the dry signal ~~level in the surrounding dry period, which we will regard as indicative of the background noise level.~~. Although the presence of ~~precipitation~~rainfall is detected unambiguously by all the instruments, the magnitude of the response differs between the links. Both the horizontally and vertically polarized detectors in the 38 GHz RAL link give very similar responses, which is expected as they receive different components of the same signal and also share a substantial part of their electric signal path, including the antenna itself. Most notable is the difference between the signal of the Nokia link and the RAL link operating at (nearly) the same frequency and polarization. Although the magnitudes are similar, the Nokia link has far less variability of the baseline signal level than all other link instruments. This difference could be caused by the differences in internal electronics of the detector. Another point of interest is that using the median of all dry data points in the 24-hour period, our estimation of the baseline signal level of the 26 GHz RAL link and to a lesser extend the 38 GHz RAL link is too high, resulting in an additive overestimation of the rain intensity. To further illustrate the great uncertainty in determining the baseline signal level even in this relatively straightforward case, Fig. 5b also shows the rain intensity corresponding to a power level equal to the 5th percentile of the dry signal. The calculated apparent ~~precipitation~~rainfall during the first peak is completely below this line, indicating that this can be regarded as noise. Regardless, the peak ~~precipitation~~rainfall estimate from the Nokia link is very close to the disdrometer estimate.

We can also see that attenuation of the microwave link signal persists for several minutes after the end of the rainfall event (according to the disdrometers) and slowly decays during this time. This could be the consequence of the link antennas becoming wet due to the rain and subsequently drying up after the event (Minda & Nakamura, 2005; Leijnse, et al., 2008).

Also plotted in Fig. 5a is the received signal level of the near-infrared link. Attenuation of this signal is indicative of visibility. In this case the visibility loss ~~seems almost entirely related to rain (~~is highly correlated with rain (correlation coefficient $r = -0.86$).

We illustrate the response of the link signals to rain with two more example events of a longer duration. One low-intensity drizzle event and one higher-intensity convective rain event with some spatial heterogeneity. On both occasions we use only the times ~~when~~for which at least one of the disdrometers indicate rain has occurred for further analyses.

The first event, on 24 November 2015, consists of a low-intensity drizzle period (intensities under 2 mm h^{-1} for most of the event) that persists for around 12 hours. The course of the event is illustrated in Fig. 6. ~~No other attenuating phenomena are found, although the~~ The RAL links show ~~a gradual shift~~some variability in the baseline power level , varying over a range of 0.11 to 0.14 dB over the course of the event~~.~~ until 13:00 hours. The Nokia link, on the other hand, stays remarkably stable during the entire event~~.~~ ranging only 0.02 dB over the same period. After that, all links show a large drop in baseline power level, with the largest magnitude in the RAL 38-GHz link (3.46 dB) and the smallest in the Nokia link (0.33 dB). Visual inspection suggests a reasonably close match in the patterns of ~~precipitation.~~rainfall. This is also reflected in Fig. 7a—d, which shows a reasonable correlation with disdrometer rain intensity for both the Nokia link and the 26-GHz RAL link (0.888 and 0.860 respectively) and less so in the 38-GHz RAL link (0.675 for vertical polarization and 0.437 for horizontal polarization). There is a strong overestimation of rain intensity from the links when compared to the spatial average of the disdrometers, both additive and multiplicative. Additive overestimation can be as high as 2.5 mm, which is more than the actual rainfall during most of the event. Additive overestimation is the least in the Nokia link-derived data, which seems to be in line with the very stable baseline. However, it is still 0.6 mm h^{-1}, which is a problem for accurately measuring accumulations from light rain events. We can also see that in this case visibility cannot be reliably used as a proxy for ~~precipitation~~rainfall intensity, as is most clearly seen after 13:00 hours.

The second event, on 4 November 2015, is ~~a~~ more spatially heterogeneous (CV = 0.64, as opposed to CV = 0.50 in the previous event.). The higher spatial heterogeneity and ~~probably~~ higher rainfall intensities suggest a convective rainfall event ~~with higher rainfall intensities~~. The total event lasts for 8 hours (see Fig. 8). Peaks in spatially-averaged rainfall intensity during this event are on the order of 20 to 30 mm h^{-1}, and individual disdrometer measurements reach up to 55 mm h^{-1}. Once again the Nokia link is remarkably stable~~,~~ (range = 0.19 dB), similarly to the 26-GHz RAL link (range = 0.33 dB), while the 38-GHz RAL link has ~~an uncertain~~a highly variable baseline~~, especially in the early part of the event.~~ (range = 1.53 dB for the horizontally polarized signal and 3.96 dB for the vertically polarized signal). During most of this event visibility seems to be a reasonable proxy for the ~~precipitation~~rainfall intensity, but drops afterwards. Correlations of link-derived rainfall with disdrometer-derived rainfall are much higher overall (r = 0.91 to r = 0.93) (Fig. 7e—h) than for the event on 24 November 2015. Additive bias is of the same order of magnitude as for the drizzle case, which means that the additive bias relative to the rainfall intensities is much less for this event than for the drizzle event. Multiplicative bias is roughly the same for all links (around a factor 1.3). The behaviour of the links between the two events is reasonably consistent.

We now compare rainfall intensities from links and from disdrometers for the entire measurement period; results are shown in Fig. 7i—l. Data points where the ~~internal Parsivel algorithm indicated no precipitation~~path-average rainfall intensity derived from the disdrometer measurements are less than 0.1 mm h^{-1} or at least one of the disdrometers indicate the presence of solid precipitation are excluded. We also exclude the period during which the link transmitters were not functioning. The Nokia link performs better than the RAL links in terms of correlations. In all cases the links significantly overestimate the rainfall intensity, both in an additive (regression intercept ranging from 0.6 to 2.0 mm h^{-1}) and a multiplicative (regression slope ranging from 1.3 to 1.7) sense. ~~There are also a number of outliers where the Parsivels register a very low amount of rain, while the links show a broad range of rainfall intensities. Note that this does not include cases where the rain as registered by the Parsivels is exactly 0 mm, because these data points are forced to zero in the link rainfall intensity retrieval algorithm. Both the general overestimation trend as well as the outliers~~The general overestimation could be attributed to attenuating

phenomena other than rain being erroneously processed as rain in the basic algorithm~~. It is less straightforward to point out an a priori cause for the few cases where underestimation occurs, but this could be due to uncertainties in the k–R relation that is used to retrieve rain.~~, in part due to the simple baseline determination process not taking these into account and because e.g. no correction was applied for wet antennas.. A similar regression in terms of specific attenuations produces nearly identical results. Therefore, we conclude that uncertainties in the *R*–*k* relation do not significantly explain uncertainties in the rainfall estimation. In typical operational settings larger temporal measurement intervals such as 15 minutes are common (e.g. Overeem, et al., 2016b). In order to illustrate the performance of a basic algorithm without any sort of correction at this resolution, Fig. 7m~~—~~p show the scatterplot and linear regression for the entire dataset, but down-sampled using a 15-minute mean. The correlation for the Nokia link is slightly lower with the 15-minute intervals than it is using 30-second intervals, yet the scatter around the regression line is also lower. In the case of the RAL links, the performance is worse for the 15-minute accumulations than for the 30-s intervals.

5.3 Solid/mixed precipitation

The microwave link precipitation detection method is principally intended for liquid precipitation. Snow and hail have different electromagnetic characteristics (i.e. ice has a different refractive index than water, and the shapes of the particles are different). Therefore different attenuation-precipitation relations hold. Non-melting snow flakes cause very little attenuation in the frequency range under study (e.g. Battan, 1973) and therefore we do not expect to be able to detect them. Wet snow hydrometeors, on the other hand, which consists of a mixture of solid and liquid water and air, generally cause more microwave attenuation than a raindrop containing the same amount of water. Since we are dealing with more complex shapes and multiple phases of water and air and therefore an inhomogeneous index of refraction, accurate estimates of wet snow attenuation and inversely, the estimation of snowfall magnitude through microwave attenuation, poses a real challenge (e.g. Paulson et al., 2011). Nevertheless, we can still detect the presence of wet snow and melting ice pellets.

Very few solid or mixed precipitation events occurred during our measurement period. Figure 9 shows one of the few snowfall occurrences during the campaign, on 4 February 2015. At this point in the campaign only one disdrometer was yet placed and no rain gauge was available, which limits the potential for a quantitative comparison. Figure 9d shows time-lapse camera footage taken during different stages of this event. The background shades in Fig. 9b indicate the type of precipitation as indicated by the Parsivel internal algorithm (blue is liquid precipitation, green is snow, red is mixed precipitation). The total event duration is about 40 minutes, yet the event is quite variable in time.

As indicated by the background colours and the camera footage, this short event starts out with a mixture of rain and ice pellets and then turns into snowfall. Along with the mixed precipitation the temperature drops from 4 °C to 1 °C. During the snowfall, the temperature drops further to 0 °C. The absolute values of the disdrometer-derived precipitation intensity ~~should~~cannot be taken ~~with a grain of salt~~at face value here, since our processing algorithm treats every particle as a raindrop. This results in far too high values during snowfall, as we do not ~~take into~~ account for the lower density of a typical snowflake. Because the disdrometer rainfall intensity shown here is that of only one disdrometer and since it was placed at one far end of the link path, we do not expect the small-scale variations to match exactly with those of the link attenuation. However, the overall dynamics of the intensity and the type of precipitation can provide some useful information.

Between 15:10 and 15:30, the links are attenuated with a magnitude that corresponds roughly with the precipitation intensity measured by the disdrometer, assuming that it is pure rain. Afterwards, when snow starts to fall between 15:30 and 15:55, the precipitation intensity derived from the disdrometers becomes a factor 10 higher than the link-derived precipitation intensity, but this is likely to be due to the faulty disdrometer algorithm when applied in snow. While both the disdrometer and the camera footage seem to indicate that the precipitation stops after 15:55, the attenuation of the links persists until the signal level returns to its initial value between 16:00 and 16:15. At this point the temperature hovers at a few tenths of degrees above zero, and the camera footage indicates some residual snow is left on the antenna covers. The snow deposits are mostly on top

of the covers and is mostly still present by 16:17, when attenuation has decayed fully so snow deposits alone cannot explain the persistent attenuation. Based on the above observations a possible explanation of the persistent attenuation effect would be the partial melting of residual snow on top of the antenna cover, which then keeps the antenna cover wet. However, further research is needed to confirm this.

Because there were few snowfall events during the entire campaign period and each of them was of short duration and mixed with other types of precipitation (similar to the event described in this section), no meaningful analyses could be done regarding the relationship between attenuation and snowfall intensity.

5.4 Temperature

Throughout the entire observation period a diurnal oscillation can be seen in the attenuation signal. This diurnal cycle is present in all signals, although the magnitude of the oscillation is in general significantly higher for the RAL links (1.0 – 1.5 dB) than it is for the Nokia link~~.~~ (~0.2 dB). The magnitude of the oscillation also varies throughout the observation period. This behaviour does not correspond to any precipitation pattern but seems to follow the known diurnal variations in temperature. Although this pattern can be seen throughout the observational period, the correlation with temperature is not always clear, because the signal is generally much weaker when other attenuating phenomena are present.

We will therefore first focus on a relatively long dry period between the 14th and 24th of April 2015, as shown in Fig. 10. During this period the disdrometers picked up no precipitation; however, the received signal levels are not constant. Instead, variations up to 1 dB are present. In Fig. 10b, the time series of ambient air temperature measured by the nearby weather station is plotted for the same period together with the visibility measured at that same station, while in Fig. 11, the power levels for this period are plotted against the temperature with a simple linear regression. We performed separate regressions for instances where humidity was above 90% and for instances where relative humidity was below 90%. This was done to distinguish instances where dew formation on the antennas might have occurred, which we will discuss in the next subsection. Also indicated in Fig. 10a are the periods where relative humidity is above 90% (green shade) and the periods where the net radiation flux at the surface is upwards (blue shade).

There is a very strong negative correlation (up to ~~–~~0.92) between received power and temperature, especially when relative humidity is below 90%, and for the most part a linear regression makes for a good fit. This is true for all the link instruments, although the slope of the linear fit is much lower for the Nokia link ~~(~~(~~–~~0.024 dB K^{-1}) than for the others (between ~~–~~0.1 and ~~–~~0.2 dB K^{-1}). Even so, the residual square error of the Nokia link regression is also lower (0.082) than those of the RAL links (~0.3). Apparently, the magnitude of the temperature dependence is very much specific to the make of the link, more so than to the frequency or polarization of operation. Similar temperature dependence of the signal was also reported by Leijnse et al. (2007) for a different microwave link instrument. The relationship between temperature and attenuation for the Nokia link breaks down at high humidity. This phenomenon is probably related to dew formation at the antennas as is discussed in more detail in ~~section~~Sect. 5.5.

In subsequent analyses we expand our investigation of a possible linear temperature dependency to the entire experimental period. However, we exclude two ~~timeframes~~time frames from this analysis. Firstly, the period between 6 August 2015 and 25 August 2015 when the transmitters ~~where~~were not functioning (but the receivers were). Secondly, we also exclude a period between 11 May 2015 and 19 May 2015 because a metal construction crane was positioned in the line of sight between the transmitter and receiver (see ~~section~~Sect. 5.7) several times in this period. The correlations and regression slopes found for this extended period are shown in Table 2 as 'whole period'.

We consider that dew-related wetting of antennas causes attenuation of the link signal, that this attenuation muddles the observed temperature dependency of the signal, and that this phenomenon seems only to occur when the nearby weather station registers a relative humidity above 90%. Therefore, we ~~must ignore~~filter the ~~data points with a relative humidity above~~

~~90%~~dataset in two more ways in order to separate temperature effects from signal attenuation in the full time period. ~~For the same reason~~First, we ~~also~~ remove all data points where the ~~Parsivel~~any disdrometer indicates any form of precipitation. Second, we remove all data points where relative humidity was above 90 %. We then find the correlations and slopes ~~as~~ indicated in Table ~~1. We see that the linear temperature dependence remains similar~~2 as 'dry only'. Furthermore, for ~~the RAL links. However, the temperature dependence~~completeness we also show correlations and slopes for a subset where, instead of the ~~Nokia link is drowned out in the noise.~~two abovementioned filters, we apply a filter that only includes periods where any of the disdrometers registered rain (shown in Table 2 as 'rain only').

~~If we do not remove the data points classified as rainy, the temperature dependence of the RAL research links is still roughly consistent. Even when we take only the data points classified as rainy, the results remain consistent.~~

We see that in the 'dry only' selection, the linear temperature dependence remains similar for the RAL links as it was for the 14—24 April selection. However, there is no evidence of a temperature dependence of the Nokia link here, even though one would expect it based on the findings from 14–24 April. We find that the correlations of the RAL link attenuations with temperature are diminished in the 'whole period' selection and further diminished in the 'rain only' case. However, they are still surprisingly high. The regression slopes found for the RAL links are all within 15% of the slopes found for the 'dry only' case using either selection.

5.5 Dew and fog

There is also another phenomenon apparent in Fig. 10, especially noticeable in the Nokia link: Some sharp drops in received power that evolve ~~in~~from midnight until the early morning (~00:00 – 05:00) and then quickly disappear again within 2 hours with peaks of 1 to 2 dB (see Fig. 10a). Comparing to Fig. 10b it is clear that they do not coincide with any change in temperature. Instead, these peaks only appear in periods when the net radiation is negative and the relative humidity is above 90%. The power gradually returns again to the previous level when the net radiation becomes positive and the event is over as soon as the relative humidity drops below 90%. From Fig. 10 we can see that these instances (where humidity is above 90%) are not correlated to temperature. These characteristics indicate that dew formation on the antennas is a plausible explanation for this phenomenon. The hypothesis is as follows: relative humidity in the air approaching 100% and a net loss of radiative energy at the surface are indicative of dew formation; water condenses on the antenna covers and builds up a thin layer of water which causes attenuation proportional to the thickness of the layer (see Leijnse et al., 2008); as the net radiative flux changes sign and the water layer dries up, the attenuation slowly returns to the baseline level.

Fog and dew often occur under the same conditions and it is therefore difficult to rule out fog as the principal cause, from correlations alone. If we take the visibility as indicative of the amount of fog, then we can see that they indeed occur often (but not always) at the same time. ~~However, the temporal patterns in the fog density within an event (Fig. 10b) are quite different than those of the detected attenuation (Fig. 10a). It is therefore most likely that this attenuation is caused by dew on the antennas.~~

In the case shown in Fig. 12 a different fog event is shown in more detail. In this case, time-lapse camera footage was available for a significant portion of the event, and is shown in Fig. 12c. Here again, strong attenuation is experienced by all the links with a peak attenuation of 3 dB in the case of the Nokia link, yet none of the disdrometers detect precipitation. Therefore, it is likely that we are dealing with a different attenuating phenomenon than precipitation. Using the basic rainfall retrieval algorithm, this event would result in an accumulated rainfall depth of 26 mm. As the time series of attenuation is smoother than we would expect of ~~precipitation~~rainfall, we are likely dealing with antenna wetting due to either dew formation, or the result of fog. The effect of fog on microwave link attenuation has also been observed by e.g. Liebe et al. (1989) and David et al. (2013). However, ~~it is debatable whether the underlying cause is the wetting of the antennas or~~ the attenuation by ~~the~~ fog droplets themselves can in this case explain only up to about 1.5 dB of attenuation. Therefore, an attribution to fog must also include the wetting of the antennas. Observation of the accompanying time-lapse camera footage (Fig. 12c) reveals

a heavy fog during the early morning which gradually clears up concurrently with the decrease in attenuation in the late morning. No camera footage was available at night during the increasing leg of the attenuation signal, because the cameras ~~were set up to not~~cannot record during low-light. However, comparison of the visibility data from the nearby weather station (Fig. 12b) with the pattern of attenuation, seems to undermine a direct relationship with fog. Visibility measurements from the NIR link along the path itself ~~is~~are of limited use in this case, since the fog is so heavy that the attenuation is 'saturated' for most of the duration. The striking correspondence of the sign switch of both net radiation and attenuation increase makes dew formation the most likely interpretation.

5.6 Wet antennas

Near the start of the measurement period a simple test case was performed to assess the effect of wet antennas on rainfall retrieval. During a dry sunny day (12 September 2014), while the ambient temperature was 21 °C, both the Nokia and the RAL 38-GHz link ~~where~~were artificially wetted in short bursts using a spray bottle. The antennas ~~where~~were wetted until saturation and then allowed to dry in the sun. In this way, the attenuating effect of wet antennas can be observed, decoupled from the attenuating effect of raindrops in air. The RAL 26-GHz link was not included in the test, as it was not yet installed at the time; however, the antenna cover design and material is identical to that of the RAL 38-GHz link (aside from its diameter) and therefore it is assumed that the effect is similar.

In Fig. 13a the resulting attenuation signal is shown. It is seen that wetting of one antenna of the Nokia link system can result in an extra attenuation of 3 to 5 dB, which is of the same order of magnitude as what is observed in dew and fog events (where presumably both antennas of a link are affected). This corresponds with a rain intensity of 15 to 22 mm h^{-1} using the power law derived in ~~section~~Sect. 4.1.3 (shown in Fig. 13b). The signal then follows an exponential decay pattern due to drying, with a decay time of 3 minutes. The RAL link response to wetting is completely different, which may be related to the way water collects on the antenna cover surface. The extra attenuation due to wetting is only 1 to 3 dB and the decay has two distinct stages. The initial peaks drop in less than a second after the spray stops, with no discernible decay pattern. However, after the initial peak, the attenuation does not drop to the baseline level; ~~I~~it stays at relatively constant elevated level after the spray. After each new spray the level may or may not change; not necessarily to a higher level. Only 21 minutes after the last spray, which was administered shortly before 14:56, has the attenuation fully decayed to the dry level (the full length of the decay is not shown on the graph). While the observations of the Nokia link conform to the theory of Minda and Nakamura (2005), which assumes a water layer of uniform thickness on the antenna, the observations of the RAL link do not. Figure 14 shows that, indeed, the assumption of a water layer of uniform thickness does not hold for the RAL link antenna cover. Instead of forming a smooth layer, the hydrophobic material of the antenna cover forces the water to either run off immediately or collect into a few large beads. The runoff leads to a reduced peak attenuation and an immediate drop afterwards, since the surface is never fully covered in water. However, the bead formation leads to a long secondary decay time, since the reduced surface to volume ratio (as compared to a uniform layer) hampers evaporation. As recorded video footage shows, with each new squirt of water, some new beads form while some others grow and fall off. The number and sizes of the beads remaining afterwards is highly variable, which might give a tentative explanation as to why the secondary attenuation level changes after each burst (and can even become lower than the previous level).

5.7 Clutter

Figure 15 shows an example of a remarkable event that occurred several times in the observation period. Figure 12a displays the received power for the four microwave link signals in the period of 10 May 2015 to 12 May 2015. There is a sudden sharp signal decrease and 18 hours later a subsequent increase towards normal levels. The disdrometers do not indicate any significant rainfall event during this time. Inspection of the time-lapse camera footage (shown in Fig. 15b) indicates that a large metal construction crane was positioned exactly in front of the link path during this time about 200 m from the receivers,

while it is positioned differently and regularly moving outside this time period. A few hours later we see another momentary drop in the received signal levels at which point the crane moves swiftly through the path. The Nokia link detects no signal loss during the long period, but it does on other similar occasions. Because the radius of the first Fresnel zone at this distance is only 1.3 m and the centres of the Nokia antennas are about 0.5 m higher than the centres of the RAL antennas, there is a distinct possibility that in some instances the obstacle was only blocking some of the links.

We see similar patterns on multiple occasions and each time a large metallic object was positioned in the path. On other occasions, for example, a window cleaners' metal gondola crane was the cause of the attenuation. These kinds of temporary obstructions of the link path cannot be ruled out in operational settings, and most of the time no continuous visual observations are available. Therefore, it would be advantageous to be able to recognise these signal patterns and remove them algorithmically.

5.8 Compound phenomena

There are several anomalies present in the dataset that cannot be easily explained by any ~~other~~single observed atmospheric phenomenon~~. It is important to take into account that there will always be unexplained anomalies~~ as described in the previous sections.

Figure 16 shows another example of a rain event. It can be seen that the link attenuation signals mimic the temporal dynamics in the rainfall. It can also be seen that the RAL 38-GHz link shows continued attenuation after the first rain event has stopped. One possible explanation could be because the antennas become wet themselves, which contributes extra to attenuation. However, the duration of the effect in this instance is almost 3 hours, which is somewhat inconsistent with the results from ~~section~~Sect. 5.6, which suggests a duration in the order of 21 minutes. It is also inconsistent with other events during this experiment when only a short attenuation period was observed after a precipitation event. Here as well, after the second rain shower, no lingering attenuation is observed. The Nokia link shows no lingering attenuation~~,~~ in both cases, which is consistent with the results from the wet antenna experiment. It is hard to specify why lingering attenuation effects occur after some rain events and not after others, but ambient conditions such as air humidity, temperature and wind speed might play a role here. The relative humidity hovers around 90% after the first event, while it drops to 80% directly after the second event. Concurrently temperature increases from 14.5 ^{o}C to 18 ^{o}C and wind speed increases from 1 m s^{-1} to 6 m s^{-1}. It is even harder to specify why some antennas are much more affected by the phenomenon than others at a given time, however the beading effect of the wet antenna with hydrophobic antenna cover might be related to this.

The examples given in this paper up till now have been simple cases where rain and other attenuating phenomena occur in an isolated fashion. These cases are important to be able to investigate and explain these phenomena. However, many times throughout the investigated period multiple phenomena have occurred simultaneously, which is a complicating factor for retrieval algorithms. Figure 17 provides an example of a complex event occurring on 1 December 2015. In this case, there is a simultaneous light drizzle and fog. Figure 17c shows that the disdrometers register rain intensities of below 1 mm h^{-1} over a period of over 4 hours. Despite the low intensity, the drizzle does produce attenuation of the links between 10:00 and 13:00, as can be seen in Fig. 17a. Fog rolls in at around 13:00 as evidenced by the time-lapse footage (not shown here) and substantiated by the increasing relative humidity and decreasing visibility as seen in Fig. 17b. From 13:00 till roughly 14:30 fog and drizzle occur simultaneously and both contribute to the attenuation. The fog~~ ~~related attenuation is most likely the effect of additional wetting of the antennas. At 15:30 the fog has blown over or has dissipated. This is captured well by the Nokia link attenuation signal. The RAL link signals remain attenuated until 20:00. This could be due to the antenna covers still being wet. As was pointed out in ~~section~~Sect. 5.6, Due to bead formation, the hydrophobic antenna covers can stay wet much longer. Indeed, from 16:00 onwards, net radiation flux is away from the surface (indicated in the shading in Fig. 17b) and thus only wind drying can take place. The simultaneous occurrence of drizzle and fog could pose a problem for binary dew filtering algorithms such as the one proposed by Overeem et al. (2016b).

6 Conclusions

Microwave attenuation—rainfall intensity relationships were determined using 30-second integrated drop size distributions obtained from 9 months of data from five laser disdrometers (and another 9 months from one disdrometer~~). . In Table 2, the determined parameters are compared with others found in the literature. The parameters found by Leijnse et al. (2010) were based on drop size distributions collected in the Netherlands as well, but were collected using filter-paper in 1968 (Wessels, 1972). We also compare with the formal ITU (International Telecommunications Union) recommendation regarding the modelling of microwave attenuation due to rain (ITU-R Recommendation, 2005). We see that the exponents (b) are very similar for the relationships obtained in this work and those obtained by Leijnse et al. (2010) and the coefficients (a) found by Leijnse et al. (2010) are somewhat lower than those found here. We can also conclude that, the a parameter is too low and the b parameter is too high in the ITU recommendation for the Dutch rainfall climatology.~~ Considering the high quality of the fits and the large amount of data for a broad range of events used to produce these fits, we recommend to use these locally-derived power laws~~.~~ for microwave link rainfall retrievals in Dutch and similar climates. We propose that analyses of disdrometer data from regions with different rainfall ~~climatologies~~climates might be used to determine the universality of these parameter values. This pertains to the coefficient a in particular, as the exponent b will always be close to one for the employed frequencies (Table 2).

In this paper we have tested a straightforward rainfall retrieval algorithm applied to the microwave link measurements on the basis of the aforementioned power-law relationship and compared the results with five disdrometers positioned along the path. This allows us to assess what the quality of a retrieval would be without taking into account the effect of other sources of attenuation. It is seen that there is a strong overestimation of rainfall intensities by the microwave links when compared to the disdrometers, when no corrections for the phenomena discussed in this paper are applied. The response of the link signals to liquid precipitation in terms of additive and multiplicative bias seems quite consistent over different types of rainfall. However, this means that drizzle is much harder to quantify than heavier rainfall events because there is an additive bias of roughly 0.6 mm h^{-1} in the Nokia link and roughly 2 mm h^{-1} in the RAL links, i.e., of the same order of magnitude as typical rainfall intensities in drizzle.

There are significant differences in the accuracy of the rainfall retrieval between the two different makes of microwave links that we used, operating at the same frequency and polarization. In general, the commercial link has a less noisy and more unambiguously interpretable signal response than the dedicated research link. The latter overestimates the rainfall intensity more during pure rainfall events, and also exhibits a stronger unintended temperature response, leading to a less stable baseline attenuation in general. The commercial link does produce a stronger overestimation due to dew. The use of a hydrophobic antenna cover should in principle reduce overestimation due to wet antennas. However, in practice, it also leads to bead formation which has adverse consequences. The beads take much longer to evaporate than a thin layer of water under similar circumstances, so after rainfall has stopped, or after dew conditions have subsided, the attenuation lingers much longer. More importantly, they make the magnitude of the attenuation during this drying-up period less predictable, because the configuration of the beads on the antennas is unpredictable. As such, we would tentatively recommend against the use of hydrophobic antenna covers for research links, although a more robust experiment might be needed to confirm this conclusion. In general, the use of two different microwave links operating at the same frequency along the same path during the same time (which should theoretically produce the same results) resulted in two remarkably different signal responses to rainfall and other attenuating phenomena. Therefore, we recommend that, when making use of data from commercial networks, note should be taken of the specific manufacturers and models the network is comprised of and the retrieval algorithm should be optimized for those link devices. This is especially relevant when parts of the network are supplied by different manufacturers. The remarkable stability of the Nokia link does, however, demonstrate the value of commercially available microwave links for precise rainfall measurements when sampled at high frequencies.

We have demonstrated the effect of several complicating phenomena in typical microwave attenuation data for rainfall retrieval. The collected data from this experiment could be used to assess the effect of different sampling strategies used by commercial microwave links from cellular communication networks in operational settings. ~~The~~Moreover, the experimental data can also be used as a test dataset to improve existing ~~operational~~ algorithms and devise corrections for the plethora of attenuating phenomena described in this paper.

Acknowledgements

The Nokia Flexihopper link system was kindly provided by T-Mobile Netherlands. The OTT Parsivel disdrometers ~~where~~were provided by Alexis Berne and colleagues from the École Polytechique Fédérale de Lausanne (EPFL) in Switzerland. The funding for this research was provided by the former Netherlands Technology Foundation STW, currently NWO-TTW (project 11944). We want to thank Pieter Hazenberg for his critical contribution to installing the instruments and Henk Pietersen for his help in the preparation for this campaign. We thank Manuel F. Rios Gaona for his contribution to the wet antenna experiment.

References

Atlas, D. and Ulbrich, C. W.: Path- and area-integrated rainfall measurement by microwave attenuation in the 1-3 cm band, J. Appl. Meteorol., 16, 1322-1331, doi: 10.1175/1520-0450(1977)016<1322:PAAIRM>2.0.CO;2, 1977.

Battan, L. J.: Radar observation of the atmosphere, University of Chicago Press, Chicago, 1973.

Beard, K.: Terminal velocity and shape of cloud and precipitation drops aloft, J. Atmos. Sci., 33, 851-864, doi: 10.1175/1520-0469(1976)033<0851:TVASOC>2.0.CO;2, 1976.

Beard, K.: Terminal velocity adjustment for cloud and precipitation drops aloft, J. Atmos. Sci., 34, 1293-1298, doi: 10.1175/1520-0469(1977)034<1293:TVAFCA>2.0.CO;2, 1977.

Berne, A., Delrieu, G., Creutin, J.-D. and Obled, C.: Temporal and spatial resolution of rainfall measurements required for urban hydrology, J. Hydrol., 299, 166-179, doi: 10.1016/j.jhydrol.2004.08.002, 2004.

Berne, A. and Uijlenhoet, R.: Path-averaged rainfall estimation using microwave links: Uncertainty due to spatial rainfall variability, Geophys. Res. Lett., 34, L07403, doi: 10.1029/2007GL029409, 2007.

Cherkassky, D., Ostrometzky, J. and Messer, H.: Precipitation classification using measurements from commercial microwave links, IEEE Trans. Geosci. Remote Sens., 52, 2350-2356, doi: 10.1109/TGRS.2013.2259832, 2014.

Chwala, C. Gmeiner, ~~a~~A., Qiu, W. Hipps, S., Nienaber, D., Siart, U., Eibert, T., Pohl, M., Seltmann, J., Fritz, J., and Kunstmann, H.: Precipitation observation using microwave backhaul links in the alpine and pre-alpine region of Southern Germany, Hydrol. Earth Syst. Sci., 16, 2647-2661, doi: 10.5194/hess-16-2647-2012, 2012.

Chwala, C., Kunstmann, H., Hipp, S. and Siart, U.: A monostatic microwave transmission experiment for line integrated precipitation and humidity remote sensing, Atmos. Res., 144, 57-72, doi: 10.1016/j.atmosres.2013.05.014, 2014.

David, N., Alpert, P. and Messer, H.: The potential of commercial microwave networks to monitor dense fog-feasibility study, J. Geophys. Res.-Atmos., 118, 750-761, doi: 10.1002/2013JD020346, 2013.

Doumounia, A., Gosset, M., Cazenave, F~~. and.~~, Kacou, M. and Zougmore, F.: Rainfall monitoring based on microwave links from cellular telecommunication networks: First results from a West African test bed, Geophys. Res. Lett., 41, 6016-6022, doi:10.1002/2014GL060724, 2014.

Holt, A., Kuznetsov, G. and Rahimi, A.: Comparison of the use of dual-frequency and single-frequency attenuation for the measurement of path-averaged rainfall along a microwave link, IEE P. Microw. Anten. P., 150, 315-320, doi: 10.1049/ip-map:20030616, 2003.

International Telecommunication Union: ITU-R Recommendation, P.838-3, Specific attenuation model for rain for use in prediction methods, 2005.

Jaffrain, J., Studzinski, A. and Berne, A.: A network of disdrometers to quantify the small-scale variability of the raindrop size distribution, Wat. Resour. Res., 47, W00H06, doi: 10.1029/2010WR009872, 2011.

Leijnse, H., Uijlenhoet, R. and Berne, A.: Errors and uncertainties in microwave link rainfall estimation explored using drop size measurements and high-resolution radar data, J. Hydrometeorol., 11, 1330-1344, doi: 10.1175/2010JHM1243.1, 2010.

Leijnse, H., Uijlenhoet, R. and Stricker, J. N. M.: Rainfall measurement using radio links from cellular communication networks, Wat. Resour. Res., 43, W03201, doi: 10.1029/2006WR005631, 2007a.

Leijnse, H., Uijlenhoet, R. and Stricker, J. N. M.: Hydrometeorological application of a microwave link: 1. Evaporation, Wat. Resour. Res., 43, W04416, doi: 10.1029/2006WR004988, 2007b.

Leijnse, H., Uijlenhoet, R. and Stricker, J. N. M.: Hydrometeorological application of a microwave link: 2. Precipitation, Wat. Resour. Res., 43, W04417, doi:10.1029/2006WR004989, 2007c.

Leijnse, H., Uijlenhoet, R. and Stricker, J. N. M.: Microwave link rainfall estimation: Effects of link length and frequency, temporal sampling, power resolution, and wet antenna attenuation, Adv. Water Resour., 31, 1481-1493, doi: 10.1016/j.advwatres.2008.03.004, 2008.

Leinonen, J.: High-level interface to T-matrix scattering calculations: Architecture, capabilities and limitations, Opt. Express, 22, 1655-1660, doi: 10.1364/OE.22.001655, 2014.

Liebe, H. J., Hufford, G. A. and Manabe, T.: A model for the complex permittivity of water at frequencies below 1 THz, Int. J. Infrared Milli., 12, 659-675, doi: 10.1007/BF01008897, 1991.

Liebe, H. J., Manabe, T. and Hufford, G. A.: Millimeter-wave attenuation and delay rates due to fog/cloud conditions, IEEE T. Antenn. Propag., 37, 1617-1612, doi: 10.1109/8.45106, 1989.

Löffler-Mang, M. and Joss, J.: An optical disdrometer for measuring size and velocity of hydrometeors, J. Atmos. Ocean. Tech., 17, 130-139, doi: 10.1175/1520-0426(2000)017<0130:AODFMS>2.0.CO;2, 2000.

Messer, H. A., Zinevich, A. and Alpert, P.: Environmental monitoring by wireless communication networks, Science, 312, 713, doi: 10.1126/science.1120034, 2006.

Mie, G.: Beiträge zur optiek trüber medien, speziell kolloidaler metallösungen, Ann. Phys. (Berl.), 330, 377-445, doi: 10.1002/andp.19083300302, 1908.

Minda, H. and Nakamura, K.: High temporal resolution path-average rain gauge with 50-GHz band microwave, J. Atmos. Ocean. Tech., 22, 165-179, doi: 10.1175/JTECH-1683.1, 2005.

Mishchenko, M. I.: Calculation of the amplitude matrix for a nonspherical particle in a fixed orientation, Appl. Opt., 39, 1026-1031, doi: 10.1364/AO.39.001026, 2000.

Mishchenko, M. I. and Travis, L. D.: Capabilities and limitations of a current FORTRAN implementation of the T-matrix method for randomly oriented, rotationally symmetric scatterers, J. Quant. Spectrosc. Ra., 60, 309-324, doi: 10.1016/S0022-4073(98)00008-9, 1998.

Mishchenko, M. I., Travis, L. D. and Mackowski, D. W.: T-matrix computations of light scattering by nonspherical particles: a review, J. Quant. Spectrosc. Ra., 55, 535-575, doi: 10.1016/0022-4073(96)00002-7, 1996.

~~Overeem, A., Leijnse, H. a~~Olson, R. L., Rogers, D. V., and Hodge, D. B.: The aR^b relation in the calculation of rain attenuation, IEEE Trans. Anten. Prop., AP-26(2), 318-329, doi: 10.1109/TAP.1978.1141845, 1978

Overeem, A., Leijnse, H. and Uijlenhoet, R.: Measuring urban rainfall using microwave links from commercial cellular communication networks, Water Resour. Res., 47, W12505, doi: 10.1029/2010WR010350, 2011.

Overeem, A., Leijnse, H. and Uijlenhoet, R.: Country-wide rainfall maps from cellular communication networks, P. Natl., Acad. Sci. USA, 110, 2741-2745, doi:10.1073/pnas.1217961110, 2013.

Overeem, A., Leijnse, H. and Uijlenhoet, R.: Retrieval algorithm for rainfall mapping from microwave link in a cellular communication network, Atmos. Meas. Tech., 9, 2425-2444, doi: 10.5194/amt-9-2425-2016, 2016a.

Overeem, A., Leijnse, H. and Uijlenhoet, R.: Two and a half years of country-wide rainfall maps using radio links from commercial cellular telecommunication networks, Water Resour. Res., 52, 8039-8065, doi: 10.1002/2016WR019412, 2016b.

~~Overeem, A., Leijnse, H. and Uijlenhoet, R.: Measuring urban rainfall using microwave links from commercial cellular communication networks, Water Resour. Res., 47, W12505, doi: 10.1029/2010WR010350, 2011.~~

Paulson, K. and Al-Mreri, A.: A rain height model to predict fading due to wet snow on terrestrial links, Radio Sci., 46, RS4010, doi: 10.1029/2010RS004555, 2011.

Rahimi, A., Holt, A., Upton, G. and Cummings, R.: Use of dual-frequency microwave links for measuring path-averaged rainfall, J. Geophys. Res. Atmos., 108, 2156-2202, doi: 10.1029/2002JD003202, 2003.

Raupach, T. and Berne, A.: Correction of raindrop size distributions measured by Parsivel disdrometers, using a two-dimensional video disdrometer as a reference, Atmos. Meas. Tech., 8, 343-365, doi: 10.5194/amt-8-343-2015, 2015.

Rios Gaona, M. F., Overeem, A., ~~Raupach, T.H., Leijnse, H., Uijlenhoet, R..: Rainfall retrieval with commercial microwave links in São Paolo, Brazil, Atmos. Meas. Tech. Discussions, doi: 10.5194/amt-2017-287, 2017.~~

~~Rios Gaona, M. F., Overeem, A.,~~ Leijnse, H. and Uijlenhoet, R.: Measurement and interpolation uncertainties in rainfall maps from cellular communication networks, Hydrol. Earth Syst. Sci., 19, 3571-3584, doi: 10.1016/j.atmosres.2011.08.011, 2015.

Rios Gaona, M. F., Overeem, A., Raupach, T.H., Leijnse, H., Uijlenhoet, R..: Rainfall retrieval with commercial microwave links in São Paolo, Brazil, Atmos. Meas. Tech. Discussions, doi: 10.5194/amt-2017-287, 2017.

Schilling, W.: Rainfall data for urban hydrology: what do we need?, Atmos. Res., 27, 5-21, doi: 10.1016/0169-8095(91)90003-F, 1991.

Schleiss, M. and Berne, A.: Identification of dry and rainy periods using telecommunication microwave links, IEEE Geosci. Remote S., 7, 611-615, doi: 10.1109/LGRS.2010.2043052, 2010.

Thurai, M., Huang, G.J., Bringi, V.N., Randeu, W.L.~~,~~. and Schönhuber, M.: Drop shapes, model comparisons, and calculations of polarimetric radar parameters in rain, J.Atmos. Ocean. Tech., 24, 1019-1032, doi: 10.1175/JTECH2051.1, 2007.

Uijlenhoet, R.: Precipitation physics and rainfall observation, in: Climate and the Hydrological Cycle, Eds.: Bierkens, M.-F.P., Dolman A.~~,~~. J., Troch, P.A., International Association of Hydrological Sciences, Wallingford, UK, 2008.

Uijlenhoet, R., Cohard, J.-M. and Gosset, M.: Path-average rainfall estimation from optical extinction measurements using a large-aperture scintillometer, J. Hydrometeorol., 12, 955-972, doi: 10.1175/2011JHM1350.1, 2011.

van der Hulst, H. C.,: Light scattering by small particles, John Wiley & Sons, New York, USA, 1957.

Vargaftik, N. B., Volkov, B. N. and Voljak, L. D.: International tables of the surface tension of water, J. Phys. Chem. Ref. Data, 12, 817-820, doi: 10.1063/1.555688, 1983.

Wang, Z., Schleiss, M., Jaffrain, J., Berne, A. and Rieckermann, J.: Using Markov switching models to infer dry and rainy periods from telecommunication microwave link signals, Atmos. Meas. Tech., 5, 1847-1859, doi: 10.5194/amt-5-1847-2012, 2012.

Waterman, P.C.: Matrix formulation of electromagnetic scattering, Proc. IEEE, 53, 805-812, doi:10.1109/PROC.1965.4058, 1965.

Wessels, H.R.A.: Metingen van regendruppels te De Bilt, scientific report W.R. 72-6, KNMI, De Bilt, The Netherlands, 1972.

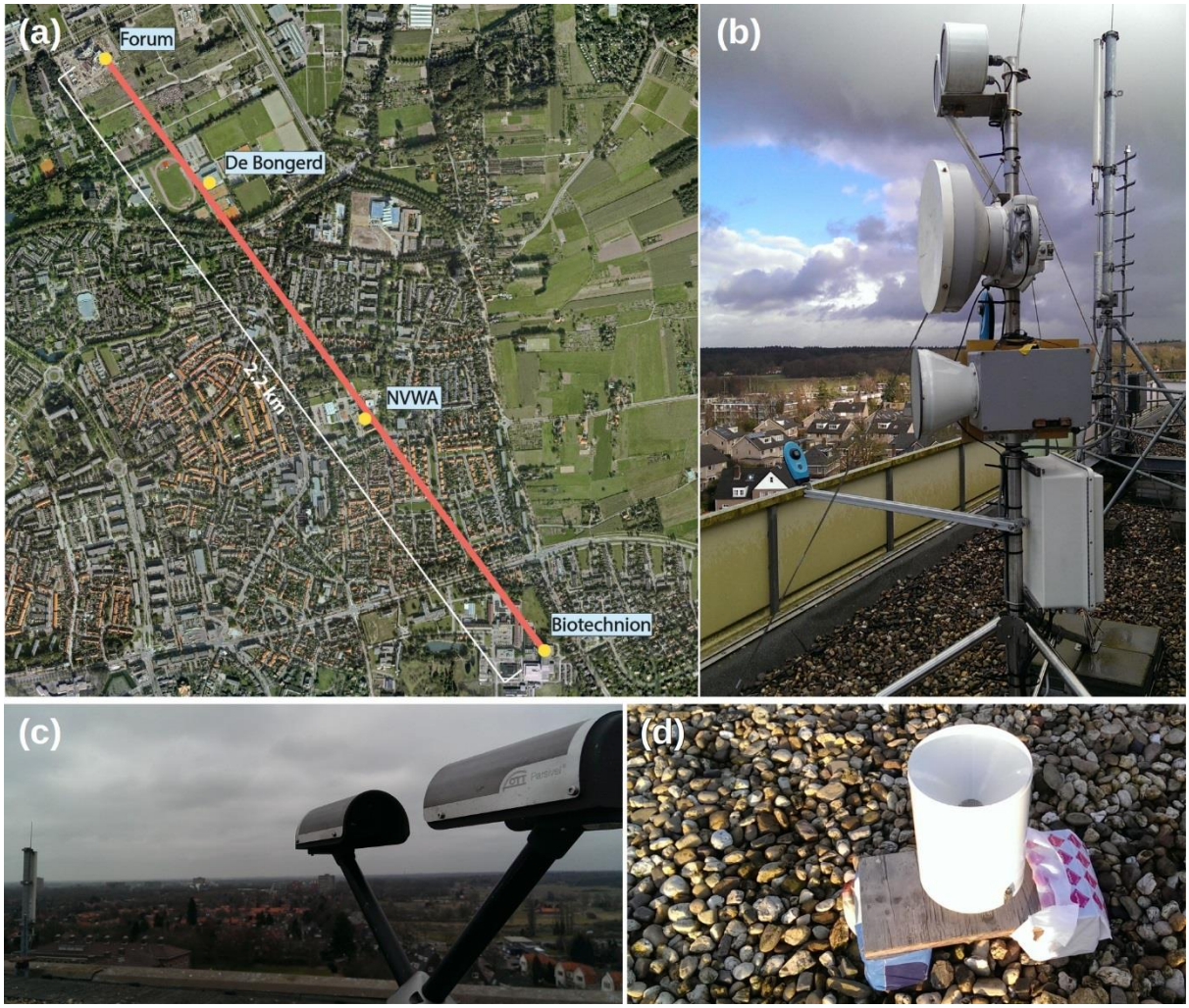

Figure 1: (a): A map of Wageningen showing the path of the links in red. The receiving antennas are at the end labelled "Forum"; the transmitting antennas are positioned at the end labelled "Biotechnion". The positions of the disdrometers are indicated with yellow dots. Each dotted position houses one disdrometer, except at the "Forum" position, where two disdrometers and an additional tipping bucket rain gauge are placed. (b): The transmitting antenna mast placed on the roof of the "Biotechnion" building. From top to bottom: Scintec BLS900, Nokia Flexihopper~~,~~ and RAL 26 GHz ~~(front),~~. The RAL 38 GHz ~~(back). ((~~is placed behind the RAL 26 GHz in the photo's perspective and thus not visible. (c): A Parsivel disdrometer (on the "Biotechnion" site). d) Précis Méchanique tipping bucket rain gauge at the "Forum" site.

Figure 2: Operational period per instrument in the experimental setup.

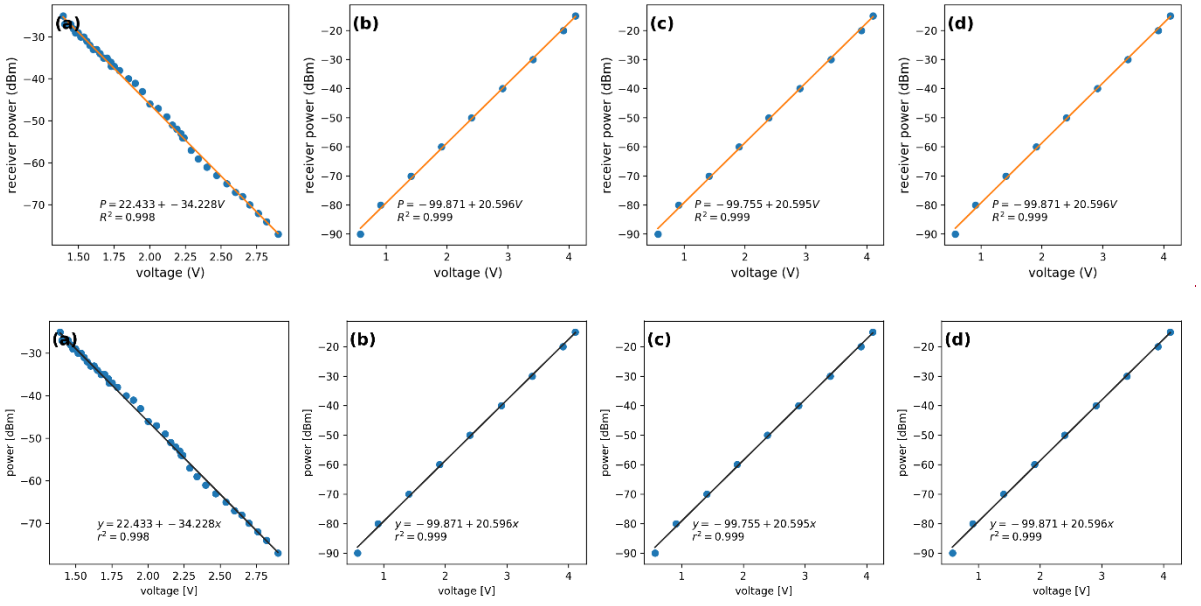

Figure 3: Received signal power versus detector voltage read-out used for the calibration of the detectors. The ~~orange~~black line indicates the fitted calibration curve. (a) Nokia ~~Flexihopper~~, (b) RAL ~~38GHz~~38 GHz horizontal, (c) RAL 38 GHz vertical, (d) RAL 26 GHz.

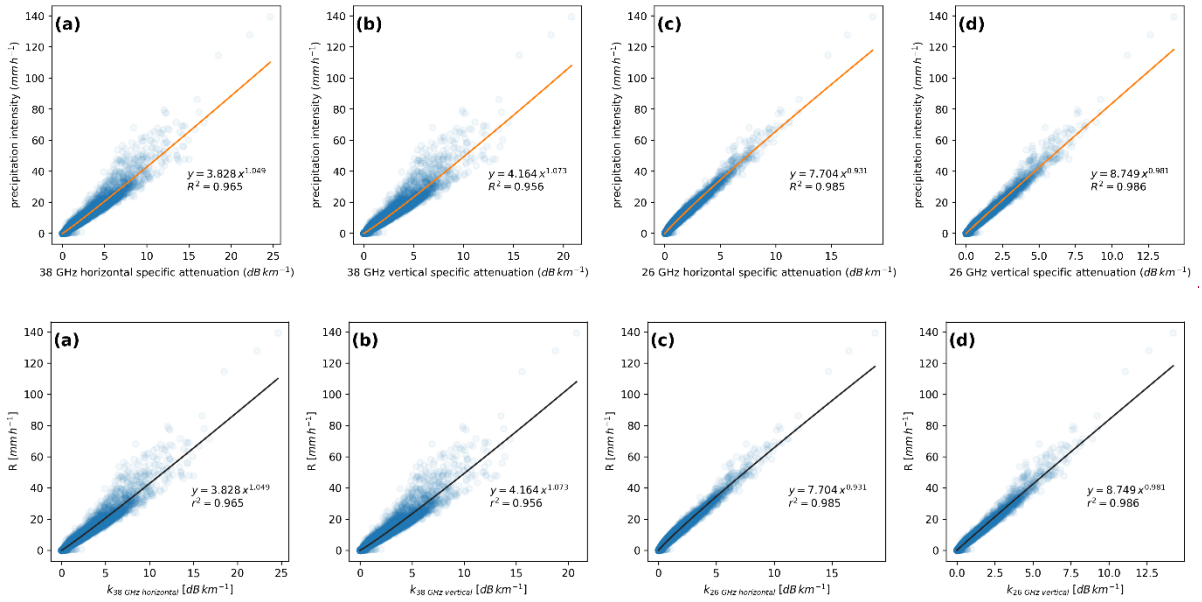

Figure 4: Disdrometer-derived ~~precipitation~~rainfall intensities plotted against disdrometer-derived specific attenuation at several frequencies and polarizations of the incident radiation. The ~~Orange lines~~black line indicates the fitted curves. (a) 38GHz horizontal, (b) 38GHz vertical, (c) 26GHz horizontal, (d) 26GHz vertical.

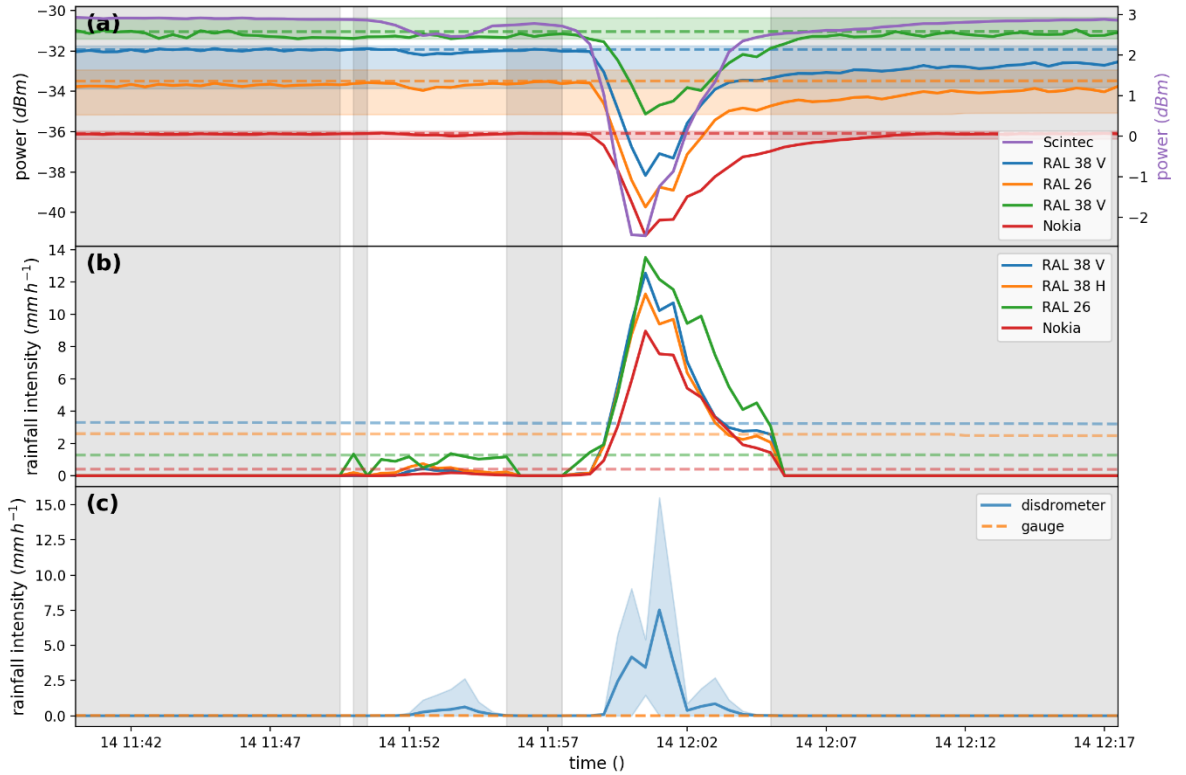

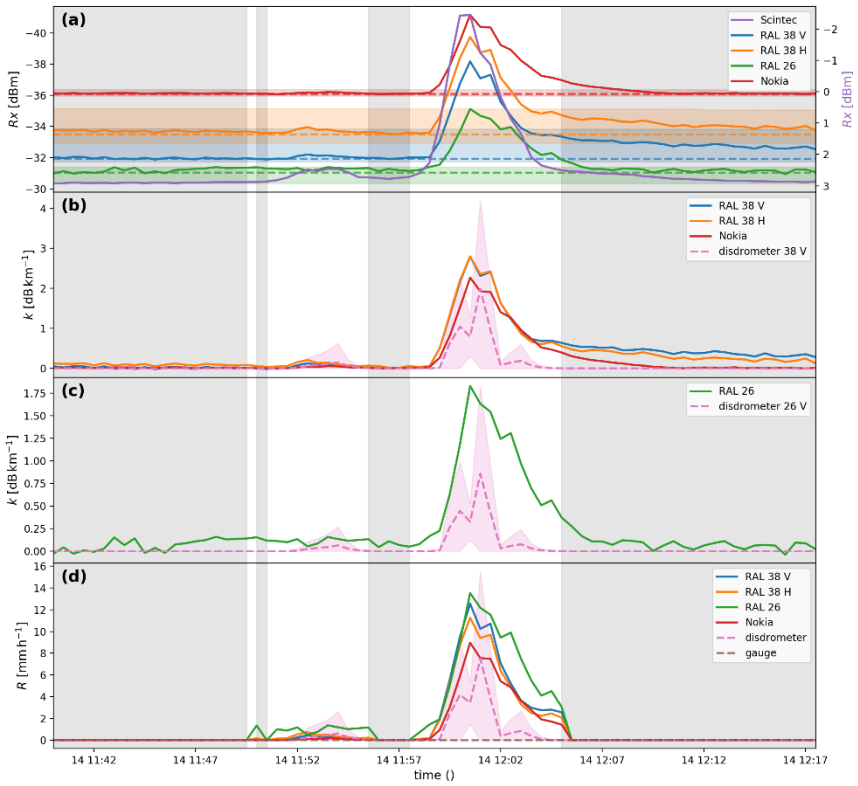

Figure 5: Time series of an event on 14 July 2015. (a): Received power levels ~~as (~~solid lines~~, with the~~) and reference levels (median over dry periods in a 24-hour moving window) ~~indicated in (~~dashed lines~~.~~). The 5th and 95th percentile power level over dry periods in a 24-~~-~~hour moving window are indicated by the coloured shading. (b): ~~Derived rainfall intensities~~ Specific attenuation of the 38-GHz links derived using the ~~basic algorithm in solid lines, dashed lines indicate~~ reference levels as well as the ~~rainfall intensity resulting from applying the k-R relationship to~~theoretical specific attenuation at 38 GHz derived from the disdrometers. Both the ~~5th percentile of the received power levels in all dry periods in the 24-hour moving window. (c): The spatial~~ weighted spatial average (dashed line) and weighted spatial standard deviation (shaded area) are shown. (c): Same as b, but for 26 GHz. (d): Rainfall intensities derived from the ~~disdrometers indicated by the blue line, with the weighted standard deviation among the~~ link attenuations using the *R–k* power law and rainfall intensities derived from the disdrometers ~~indicated with~~. Both the ~~light blue~~ weighted spatial average (dashed line) and weighted spatial standard deviation (shaded area) are indicated. The rainfall intensities derived from the tipping bucket gauge are indicated with the brown dashed line. Dry periods, as ~~indicated by~~determined with the disdrometers, are ~~indicated with~~ represented by grey shaded areas.

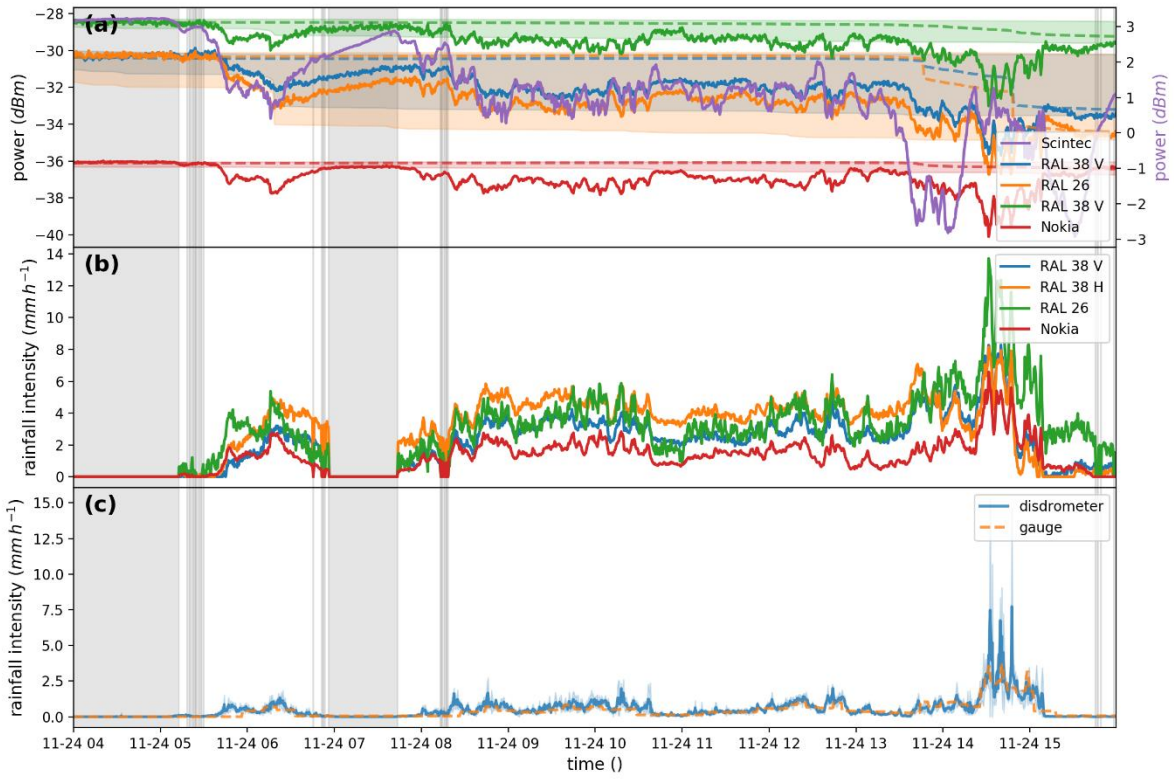

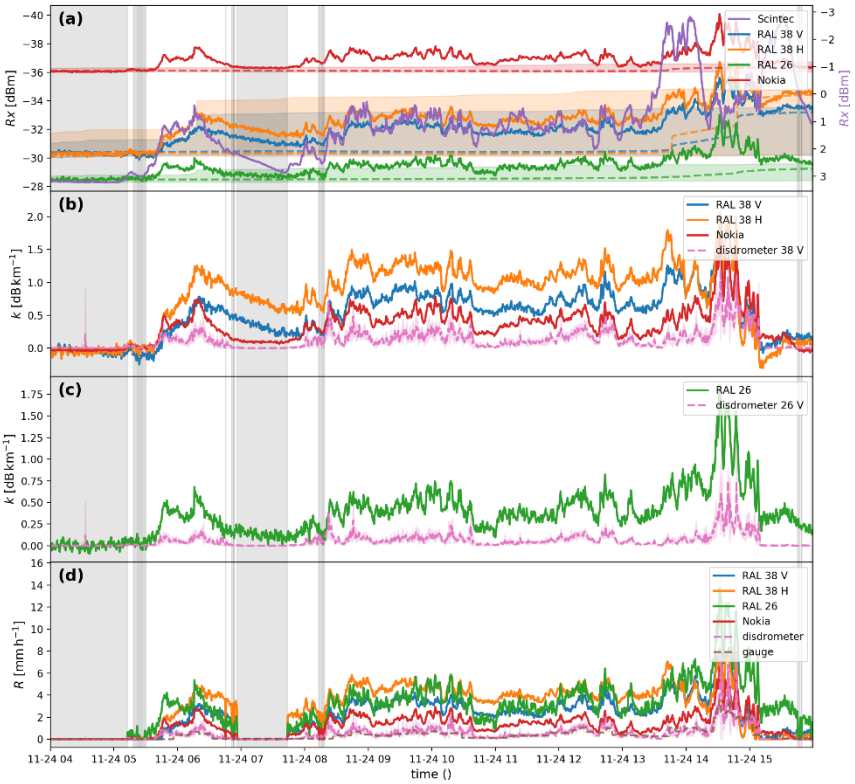

Figure 6: Time series of an event on 24 November 2015. (a): Received power levels ~~as~~ (solid lines~~, with the~~) and reference levels (median over dry periods in a 24-~~-~~hour moving window) ~~indicated with~~ (dashed lines~~.~~). The 5th and 95th percentile power levels over dry periods in a 24-~~-~~hour moving window are indicated by the coloured shading. ~~(b): Derived rainfall intensities using the basic algorithm in solid lines.~~(b): Specific attenuation of the 38-GHz links derived using the reference levels as well as the theoretical specific attenuation at 38 GHz derived from the disdrometers Both the weighted spatial average (dashed line) and weighted spatial standard deviation (shaded area) are shown. (c): ~~The spatial weighted average~~ Same as b, but for 26 GHz. (d): Rainfall intensities derived from the link attenuations using the *R*–*k* power law and rainfall intensities derived from the disdrometers ~~indicated by the blue line, with~~. Both the weighted spatial average (dashed line) and weighted spatial standard deviation ~~among the disdrometers indicated with the light blue~~ (shaded area) are shown. The rainfall intensities derived from the tipping bucket gauge are indicated with the brown dashed line. Dry periods, as ~~indicated by~~determined with the disdrometers, are ~~indicated with~~ represented by grey shaded areas.

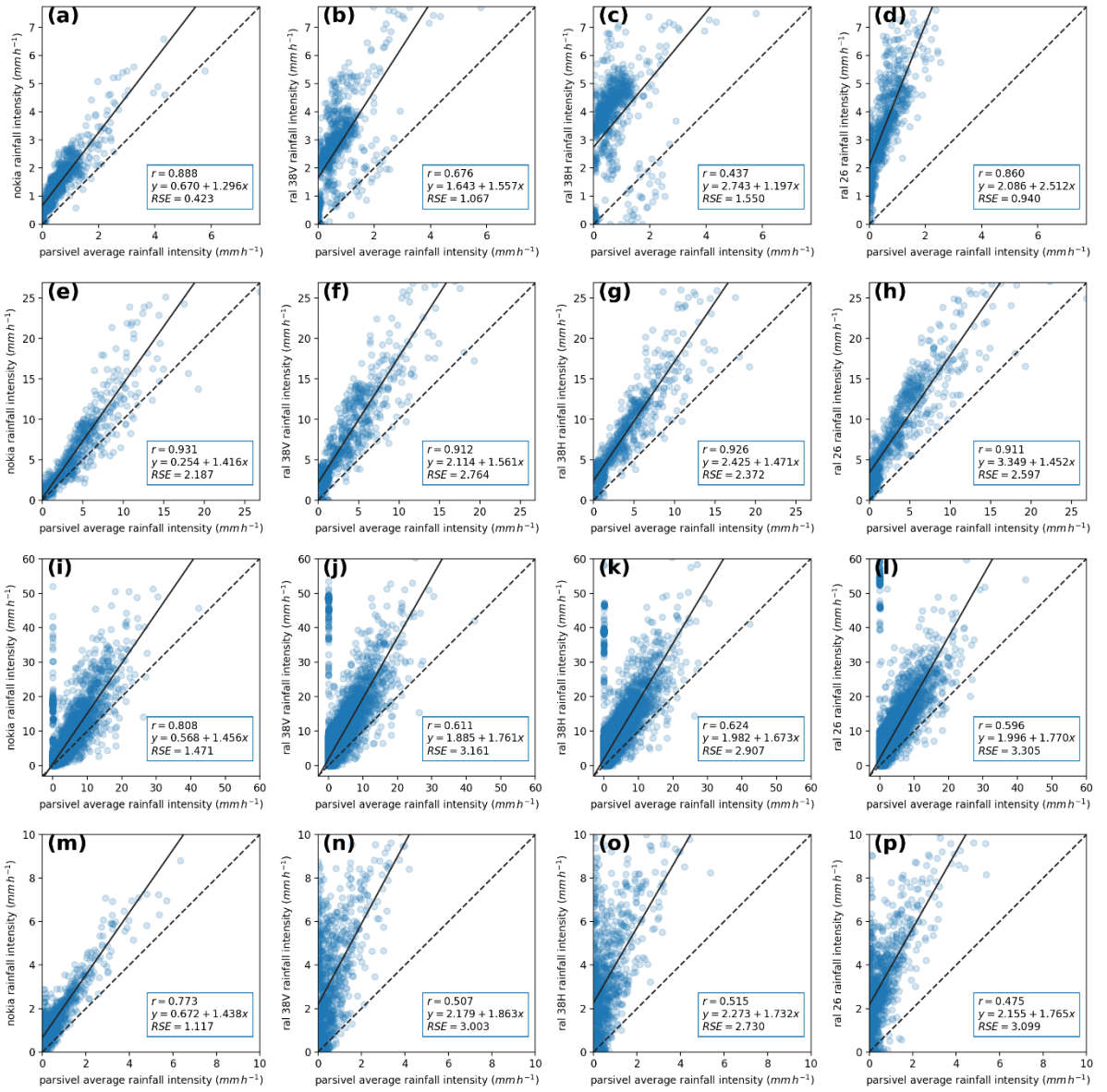
(a)
nokia rainfall intensity ($mm\,h^{-1}$)
$r = 0.888$
$y = 0.670 + 1.296x$
$RSE = 0.423$
parsivel average rainfall intensity ($mm\,h^{-1}$)
(b)
ral 38V rainfall intensity ($mm\,h^{-1}$)
$r = 0.676$
$y = 1.643 + 1.557x$
$RSE = 1.067$
parsivel average rainfall intensity ($mm\,h^{-1}$)
(c)
ral 38H rainfall intensity ($mm\,h^{-1}$)
$r = 0.437$
$y = 2.743 + 1.197x$
$RSE = 1.550$
parsivel average rainfall intensity ($mm\,h^{-1}$)
(d)
ral 26 rainfall intensity ($mm\,h^{-1}$)
$r = 0.860$
$y = 2.086 + 2.512x$
$RSE = 0.940$
parsivel average rainfall intensity ($mm\,h^{-1}$)
(e)
nokia rainfall intensity ($mm\,h^{-1}$)
$r = 0.931$
$y = 0.254 + 1.416x$
$RSE = 2.187$
parsivel average rainfall intensity ($mm\,h^{-1}$)
(f)
ral 38V rainfall intensity ($mm\,h^{-1}$)
$r = 0.912$
$y = 2.114 + 1.561x$
$RSE = 2.764$
parsivel average rainfall intensity ($mm\,h^{-1}$)
(g)
ral 38H rainfall intensity ($mm\,h^{-1}$)
$r = 0.926$
$y = 2.425 + 1.471x$
$RSE = 2.372$
parsivel average rainfall intensity ($mm\,h^{-1}$)
(h)
ral 26 rainfall intensity ($mm\,h^{-1}$)
$r = 0.911$
$y = 3.349 + 1.452x$
$RSE = 2.597$
parsivel average rainfall intensity ($mm\,h^{-1}$)
(i)
nokia rainfall intensity ($mm\,h^{-1}$)
$r = 0.808$
$y = 0.568 + 1.456x$
$RSE = 1.471$
parsivel average rainfall intensity ($mm\,h^{-1}$)
(j)
ral 38V rainfall intensity ($mm\,h^{-1}$)
$r = 0.611$
$y = 1.885 + 1.761x$
$RSE = 3.161$
parsivel average rainfall intensity ($mm\,h^{-1}$)
(k)
ral 38H rainfall intensity ($mm\,h^{-1}$)
$r = 0.624$
$y = 1.982 + 1.673x$
$RSE = 2.907$
parsivel average rainfall intensity ($mm\,h^{-1}$)
(l)
ral 26 rainfall intensity ($mm\,h^{-1}$)
$r = 0.596$
$y = 1.996 + 1.770x$
$RSE = 3.305$
parsivel average rainfall intensity ($mm\,h^{-1}$)
(m)
nokia rainfall intensity ($mm\,h^{-1}$)
$r = 0.773$
$y = 0.672 + 1.438x$
$RSE = 1.117$
parsivel average rainfall intensity ($mm\,h^{-1}$)
(n)
ral 38V rainfall intensity ($mm\,h^{-1}$)
$r = 0.507$
$y = 2.179 + 1.863x$
$RSE = 3.003$
parsivel average rainfall intensity ($mm\,h^{-1}$)
(o)
ral 38H rainfall intensity ($mm\,h^{-1}$)
$r = 0.515$
$y = 2.273 + 1.732x$
$RSE = 2.730$
parsivel average rainfall intensity ($mm\,h^{-1}$)
(p)
ral 26 rainfall intensity ($mm\,h^{-1}$)
$r = 0.475$
$y = 2.155 + 1.765x$
$RSE = 3.099$
parsivel average rainfall intensity ($mm\,h^{-1}$)

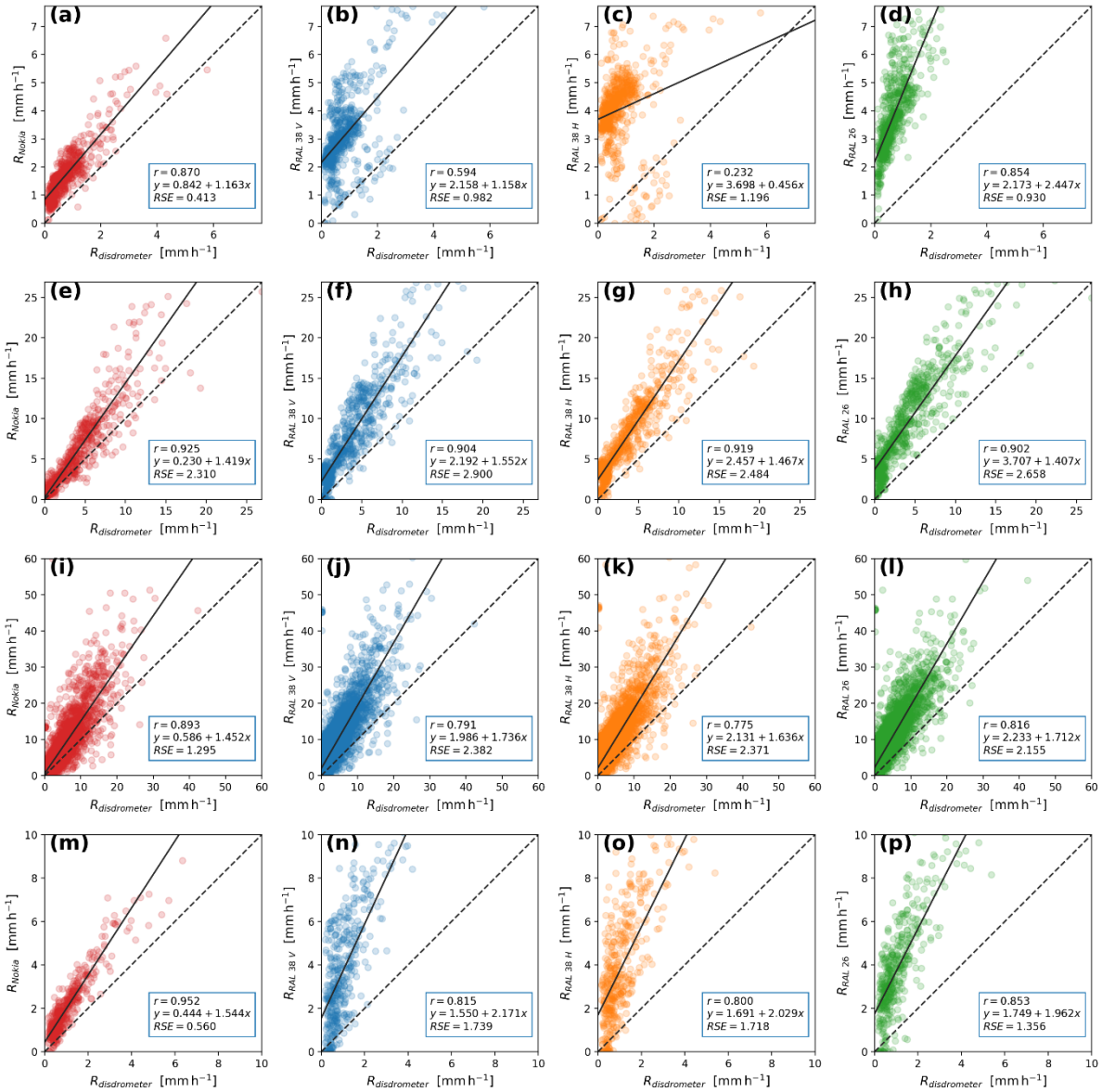

Figure 7: Scatterplots of link-derived rainfall intensities versus disdrometer-derived rainfall intensities. Solid lines indicate a linear least-squares fit, dotted lines indicate the 1:1 line. Within each plot the correlation coefficient (*r*), the fitted line function and the residual standard error (RSE) are also shown. Links from left to right: Nokia, RAL ~~38GHz~~38 GHz vertical, RAL ~~38GHz~~38 GHz horizontal, RAL 26GHz. From top to bottom: 24 November 2015 (down-sampled to 30 s), 4 November 2015 (down-sampled to 30 s), whole dataset down-sampled to 30 s, whole dataset down-sampled to 15 min.

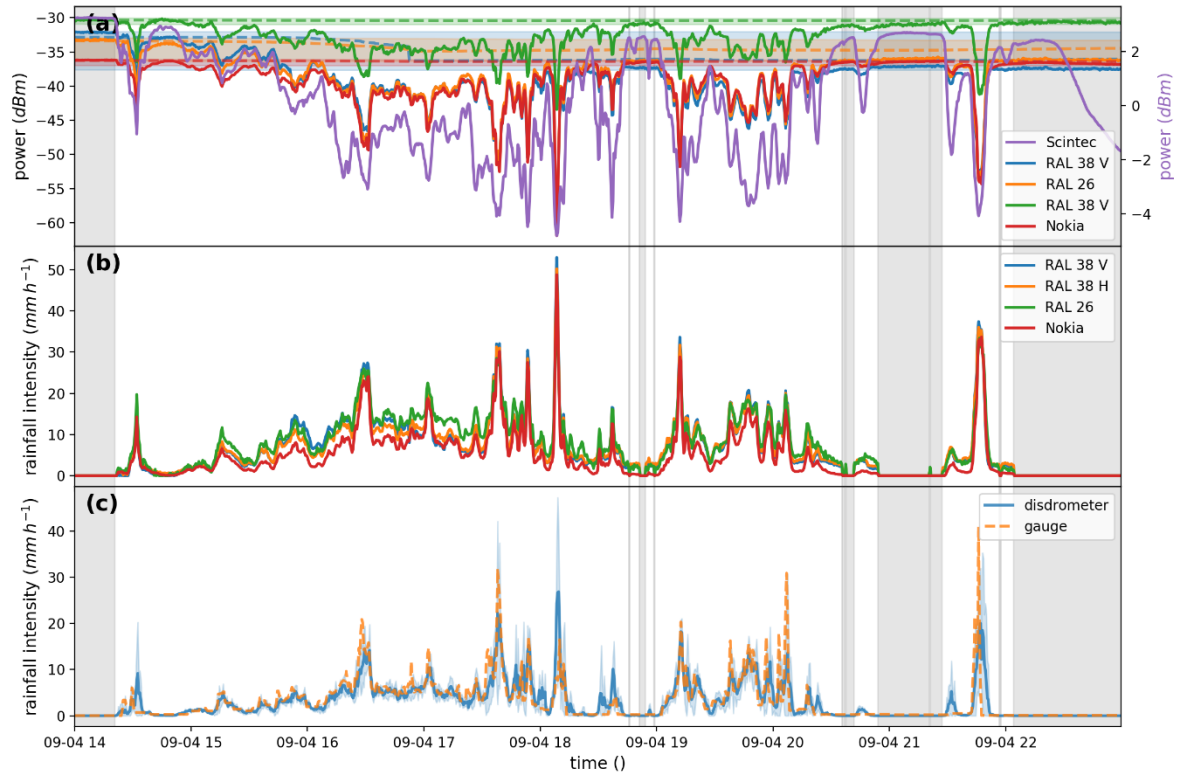

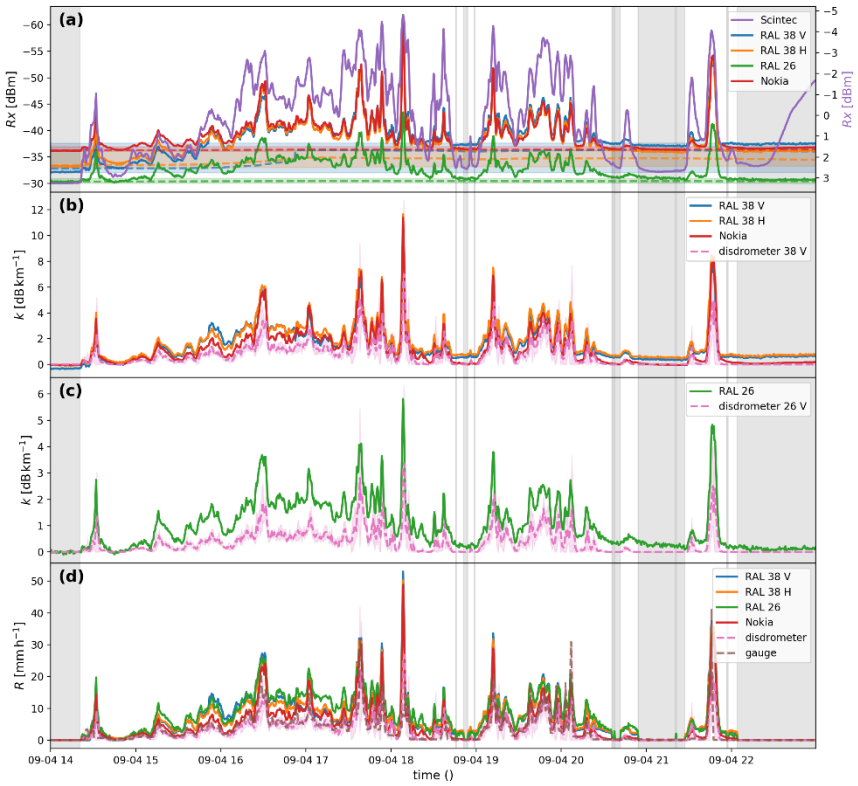

Figure 8: Time series of an event on 4 November 2015. (a): Received power levels ~~at the detectors as (~~solid lines~~, with the~~) and reference levels (median over dry periods in a 24~~–~~hour moving window) ~~indicated by (~~dashed lines~~.~~). The 5th and 95th percentile power ~~levels~~level over dry periods in a 24~~–~~hour moving window are indicated by the coloured shading. (b): ~~Derived rainfall intensities~~ Specific attenuation of the 38-GHz links derived using the ~~basic algorithm in solid. (c): The spatial~~ reference levels as well as the theoretical specific attenuation at 38 GHz derived from the disdrometers. Both the weighted spatial average (dashed line) and weighted spatial standard deviation (shaded area) are shown. (c): Same as b, but for 26 GHz. (d): Rainfall intensities derived from the link attenuations using the *R*–*k* power law and rainfall intensities derived from the disdrometers ~~indicated by the blue line, with~~. Both the weighted spatial average (dashed line) and weighted spatial standard deviation ~~among the disdrometers indicated with the light blue (~~shaded area~~)~~ are shown. The rainfall intensities derived from the tipping bucket gauge are indicated with the brown dashed line. Dry periods, as ~~indicated by~~determined with the disdrometers, are ~~indicated with~~ represented by grey shaded areas.

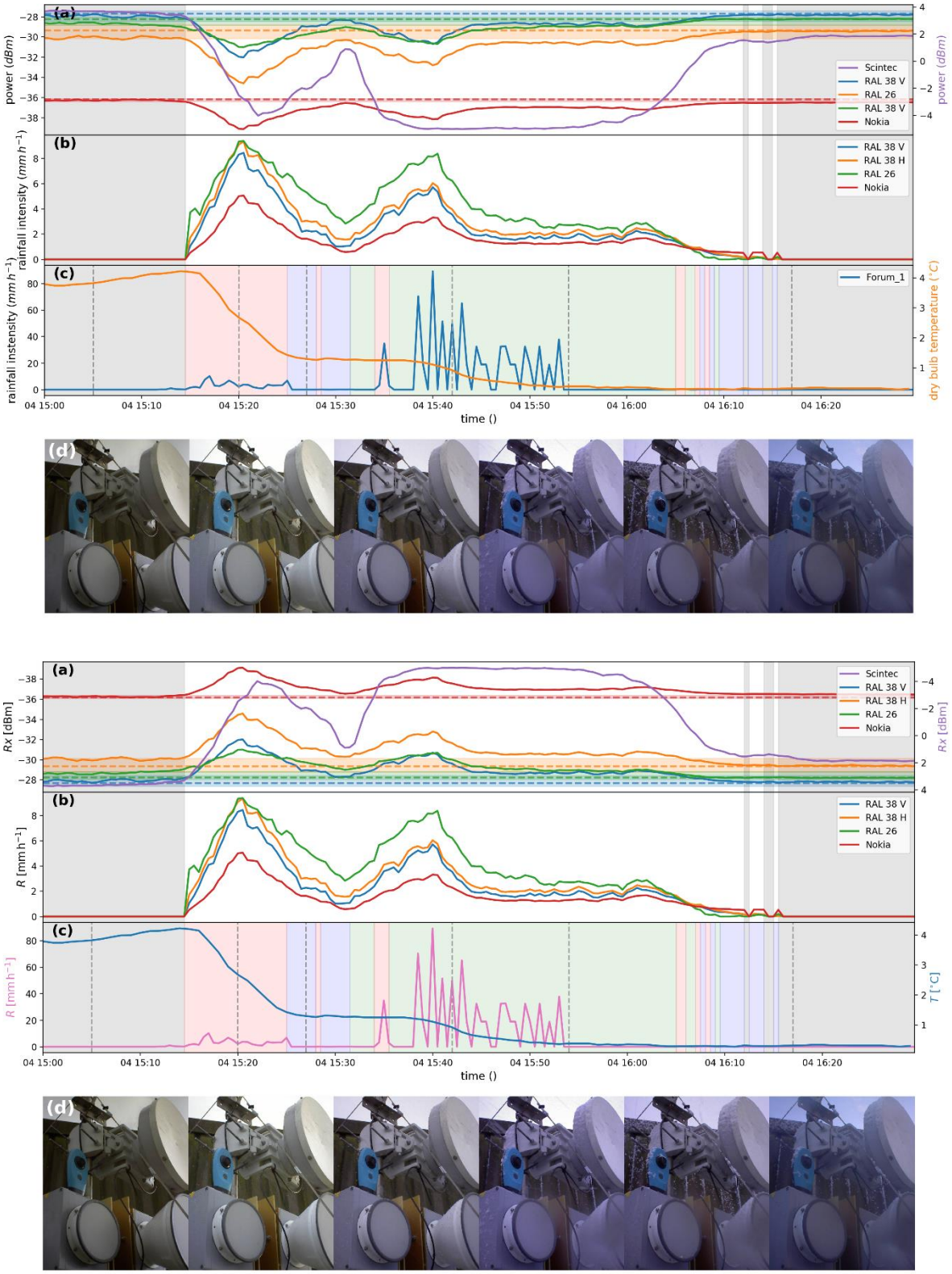

Figure 9: Time series of an event on 4 February 2015. (a): Received power levels at the detectors ~~as~~ (solid lines~~, with the~~) and reference levels (median over dry periods in a 24 hour moving window) ~~indicated by~~ (dashed lines~~.~~). The 5th and 95th percentile power levels over dry periods in a 24~~-~~hour moving window are indicated by the coloured shading. (b): Derived rainfall intensities using the basic algorithm ~~in solid lines.~~ (c): Rainfall intensities derived from the disdrometer positioned at "Forum" ~~indicated by a blue line;~~and ambient air temperature at 2 m at the "Veenkampen" meteorological station ~~indicated by an orange line.~~. Dry periods, as ~~indicated by~~determined with the disdrometers, are ~~indicated with~~ represented by grey shaded areas. Periods with mixed precipitation are indicated with red shaded areas; periods where only liquid precipitation is detected are indicated in blue and periods with snow are indicated in green. (d): Images from the time-lapse camera at the location of the transmitting antennas aimed at the antennas. The times at which these images ~~where~~were captured ~~is~~are indicated by the vertical dashed lines~~.~~ in (c).

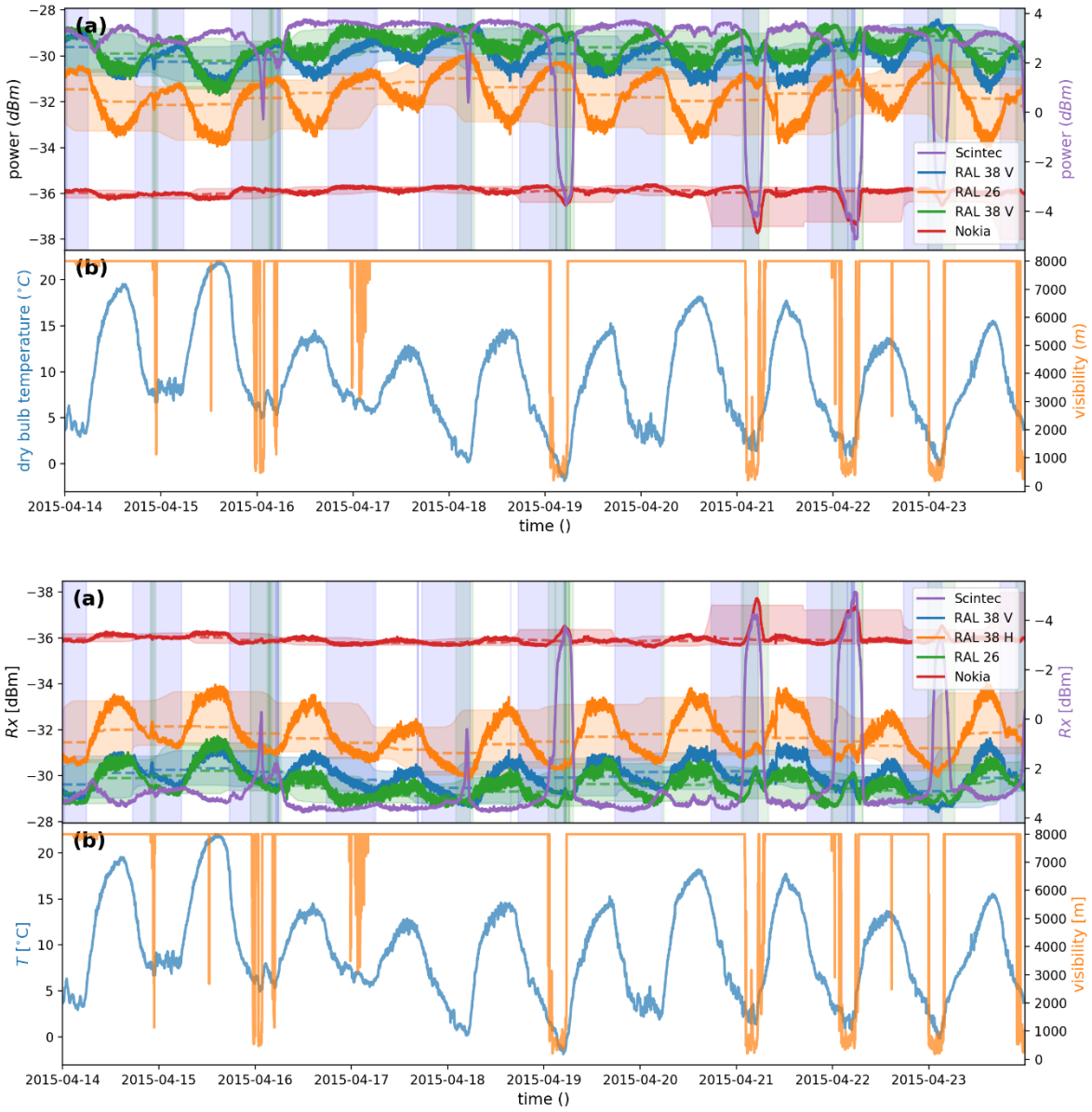

Figure 10: Time series of the period between 14 April 2015 and 24 April 2015. (a): Received power levels ~~as~~ (solid lines~~, with the~~) and reference levels (median over dry periods in a 24-hour moving window) ~~indicated by~~ (dashed lines~~.~~). Periods with a negative net radiation flux at the surface are indicated with blue shading. Periods with a relative humidity >90% are indicated with green shading. (b): Several atmospheric variables measured at the "Veenkampen" meteorological station: visibility and ambient air temperature at 2 m indicated with orange and blue lines, respectively.

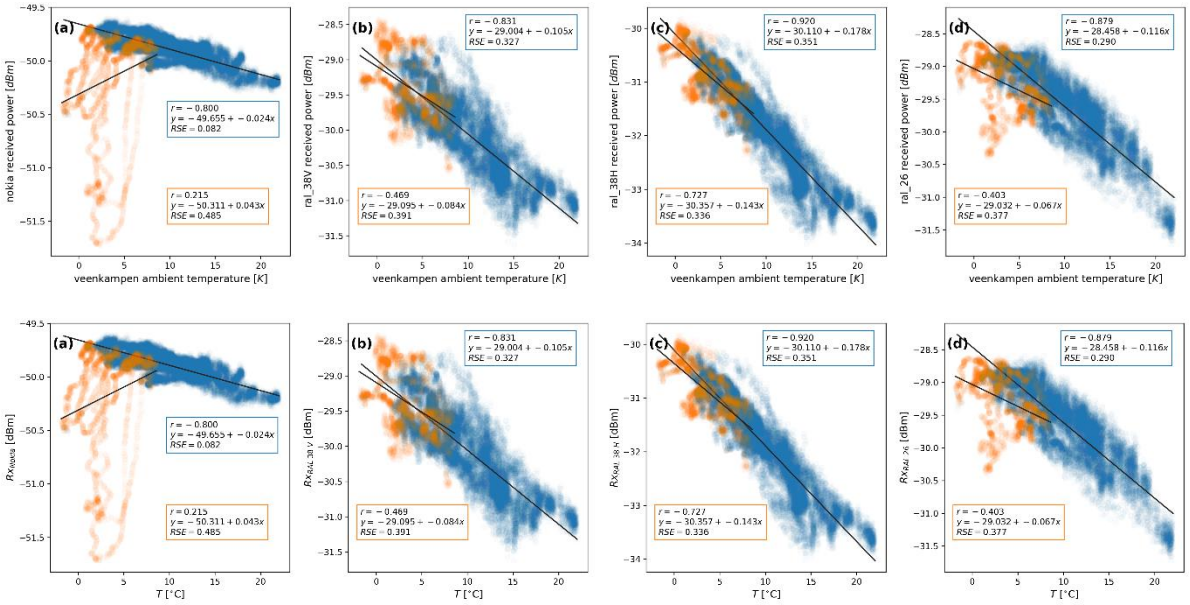

Figure 11: Scatterplots of link received power versus ambient air temperature measured at the "Veenkampen" meteorological station. Blue dots indicate times when relative humidity (as measured at "Veenkampen") is < 90%; orange dots indicate times when relative humidity > 90%. Solid lines indicate linear least-squares regression fit. Links: (a) Nokia Flexihopper, (b) RAL ~~38GHz~~38 GHz vertical, (c) RAL ~~38GHz~~38 GHz horizontal, (d) RAL 26GHz.

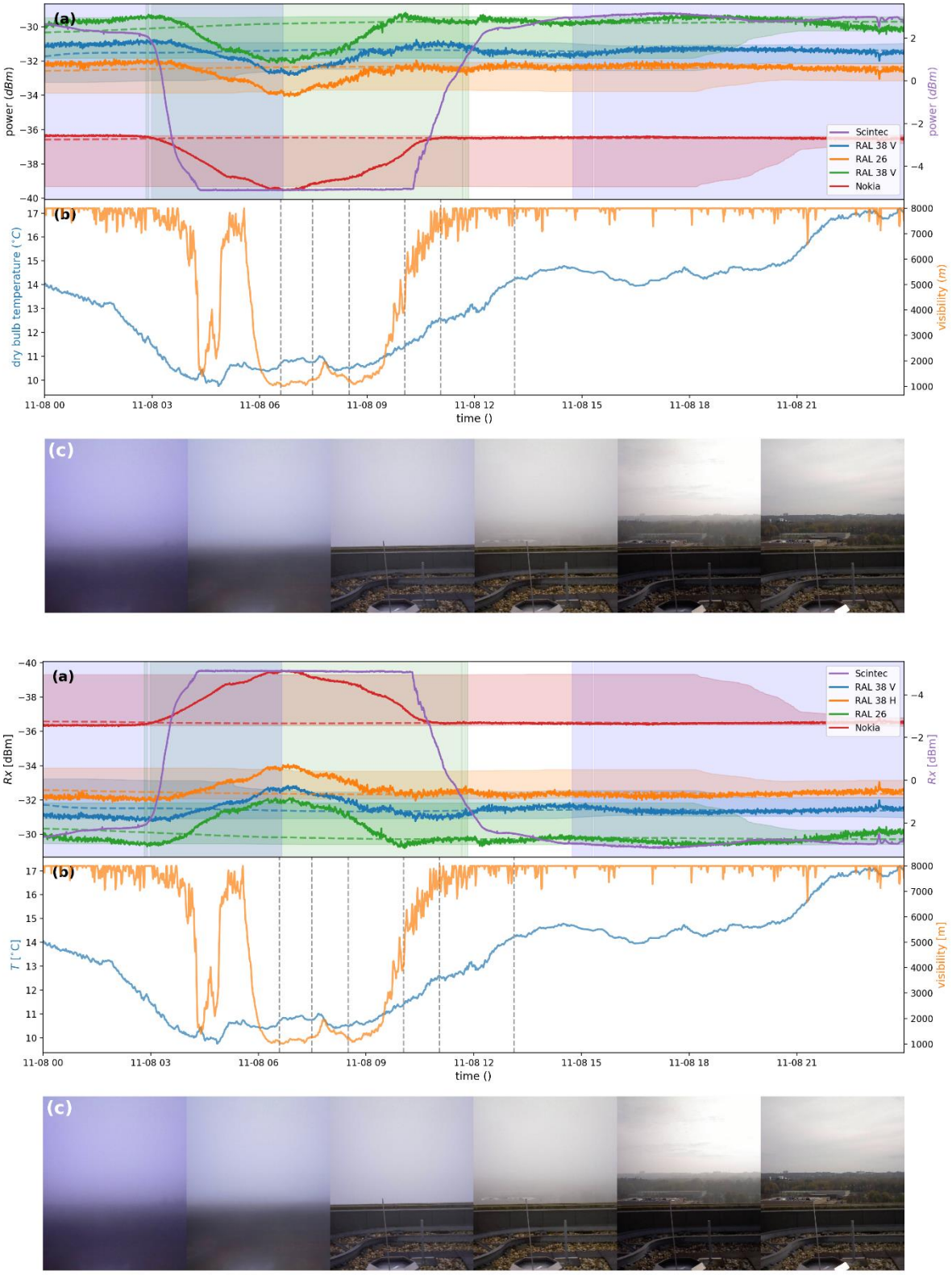

Figure 12: Time series of an event on 8 November 2015. (a): Received power levels at the detectors ~~as~~ (solid lines~~, with the~~) and reference levels (median over dry periods in a 24-hour moving window) ~~indicated by~~ (dashed lines~~.~~). Periods with a negative net radiation flux at the surface are indicated with blue shading. Periods with a relative humidity >90% are indicated with green shading. (b): Several atmospheric variables measured at the "Veenkampen" meteorological station: visibility and ambient air temperature at 2 m indicated with orange and blue lines, respectively. (c): Images from the time-lapse camera at the location of the receiving antennas aimed along the link path. The times at which these images ~~where~~were captured ~~is~~are indicated by the vertical dotted lines.

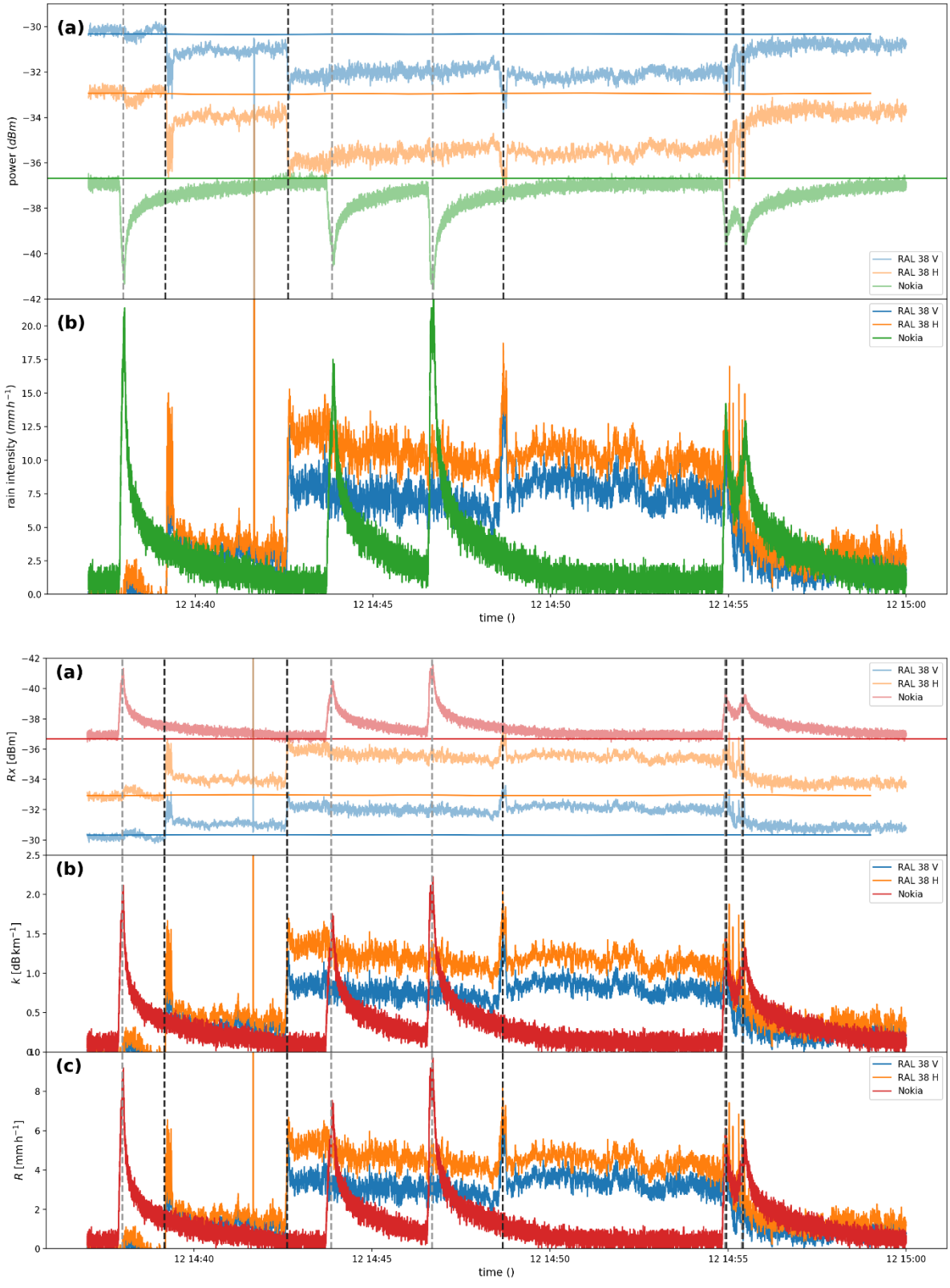

Figure 13: Time series of the wet antenna experiment on 12 September 2014. (a): Received power levels at the detectors, with the reference levels indicated in darker hues. The reference levels are singular values manually fitted for this event. These are the raw 20-Hz sampled data, not the 30–second resampled data. The dotted vertical lines indicate the moments when a water spray was applied, with the dark grey lines indicating sprays on the RAL antenna and the light grey lines indicating sprays on the Nokia antenna. (b): Specific attenuation of the links. (c): Derived rainfall intensities using the ~~basic algorithm~~ *R*–*k* power law.

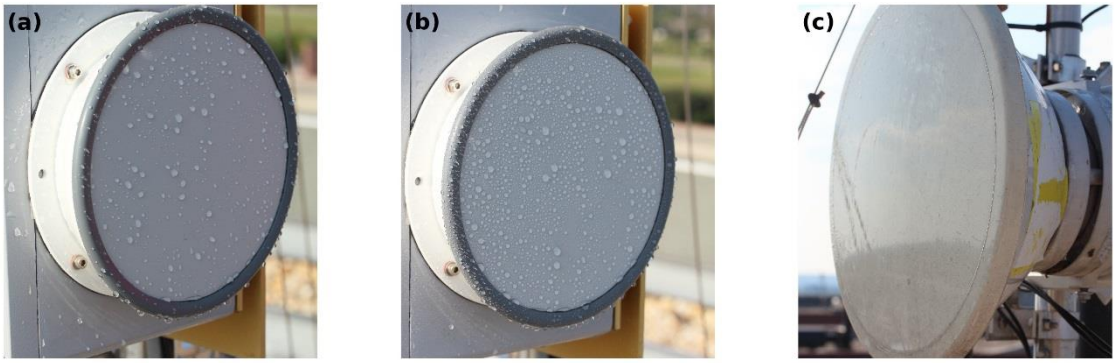

Figure 14: Photographs of the receiving antenna covers during the wet antenna experiment taken just after the antennas ~~where~~were sprayed. (a) and (b) are two instances of the RAL ~~38GHz~~38-GHz cover. (c) is the Nokia Flexihopper cover.

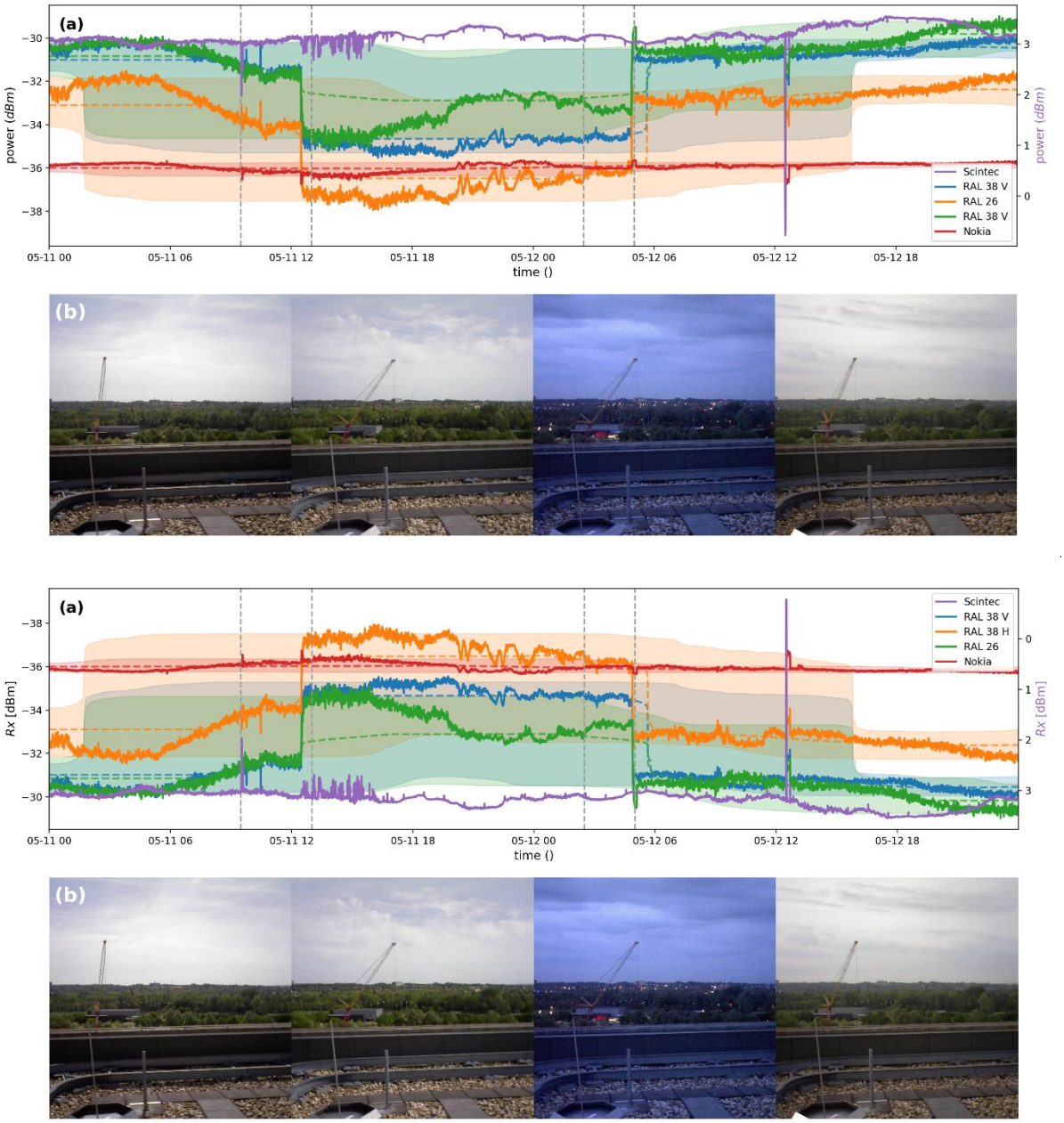

Figure 15: Time series of an event on 11 May 2015. (a): Received power levels at the detectors as solid lines, with the reference levels (median over dry periods in a 24-hour moving window) indicated by dashed lines. The 5th and 95th percentile power levels over dry periods in a 24-hour moving window are indicated by the coloured shading. (b): Images from the time-lapse camera at the location

of the receiving antennas aimed ~~-~~along the link path. The times at which these images were captured is indicated by the vertical dotted lines.

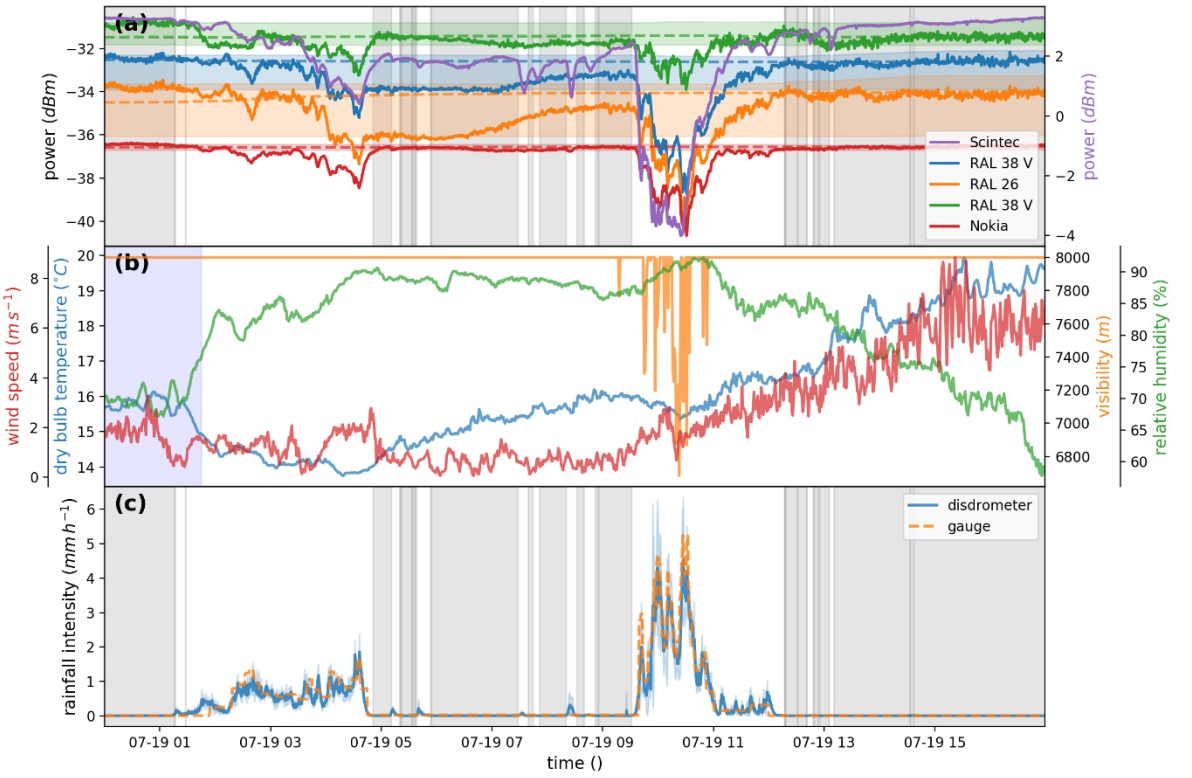

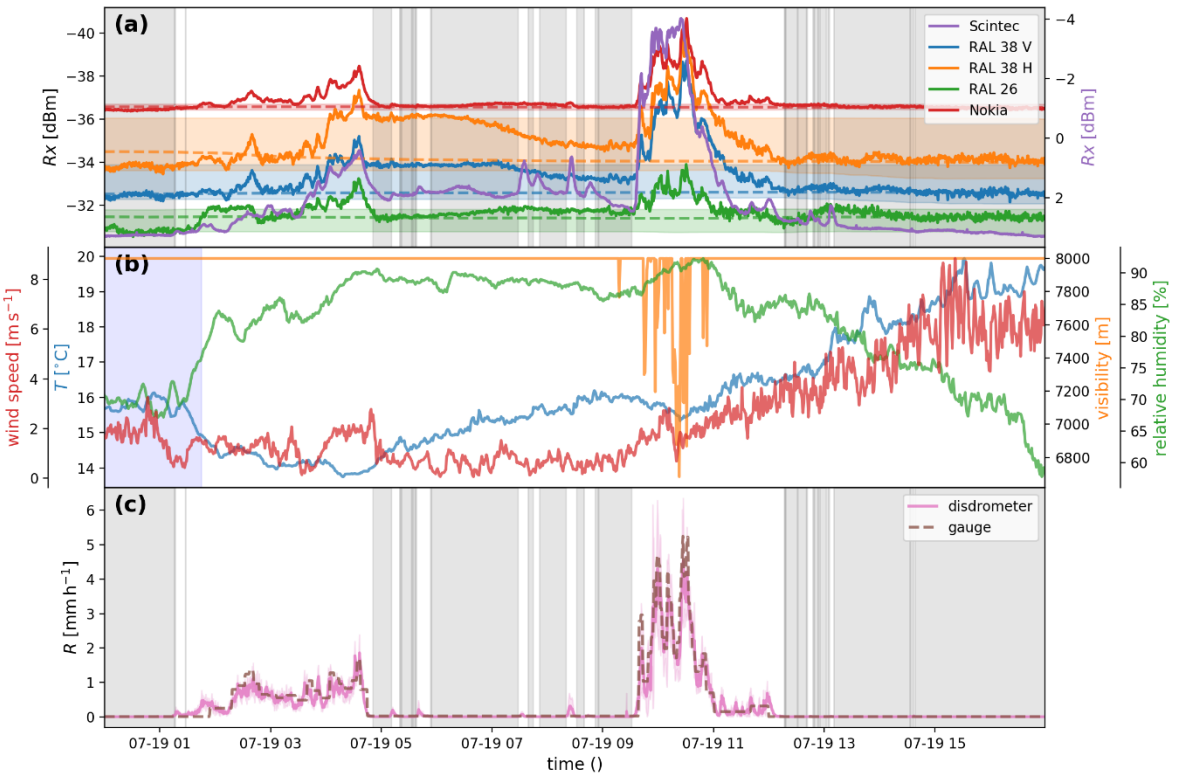

Figure 16: Time series of an event on 19 July 2015. (a): Received power levels at the detectors ~~as~~ (solid lines~~, with the~~) and reference levels (median over dry periods in a 24~~-~~-hour moving window) ~~indicated by~~ (dashed lines~~.~~). The 5th and 95th percentile power levels over dry periods in a 24~~-~~-hour moving window are indicated by the coloured shading. (b): Several atmospheric variables measured at the "Veenkampen" meteorological station: relative humidity, visibility~~ and,~~ ambient air temperature at 2 m and wind speed indicated with blue, orange~~ and,~~ green and red lines, respectively. Periods with a negative net radiation flux at the surface are indicated with blue shading. (c): The spatial weighted average rainfall intensities derived from the disdrometers indicated by the ~~blue~~pink line, with the weighted standard deviation among the disdrometers ~~indicated with~~displayed by the ~~light blue~~pink shaded

area. The rainfall intensities derived from the tipping bucket gauge indicated with the dashed line. Dry periods, as indicated by the disdrometers, are ~~indicated with~~displayed by grey shaded areas.

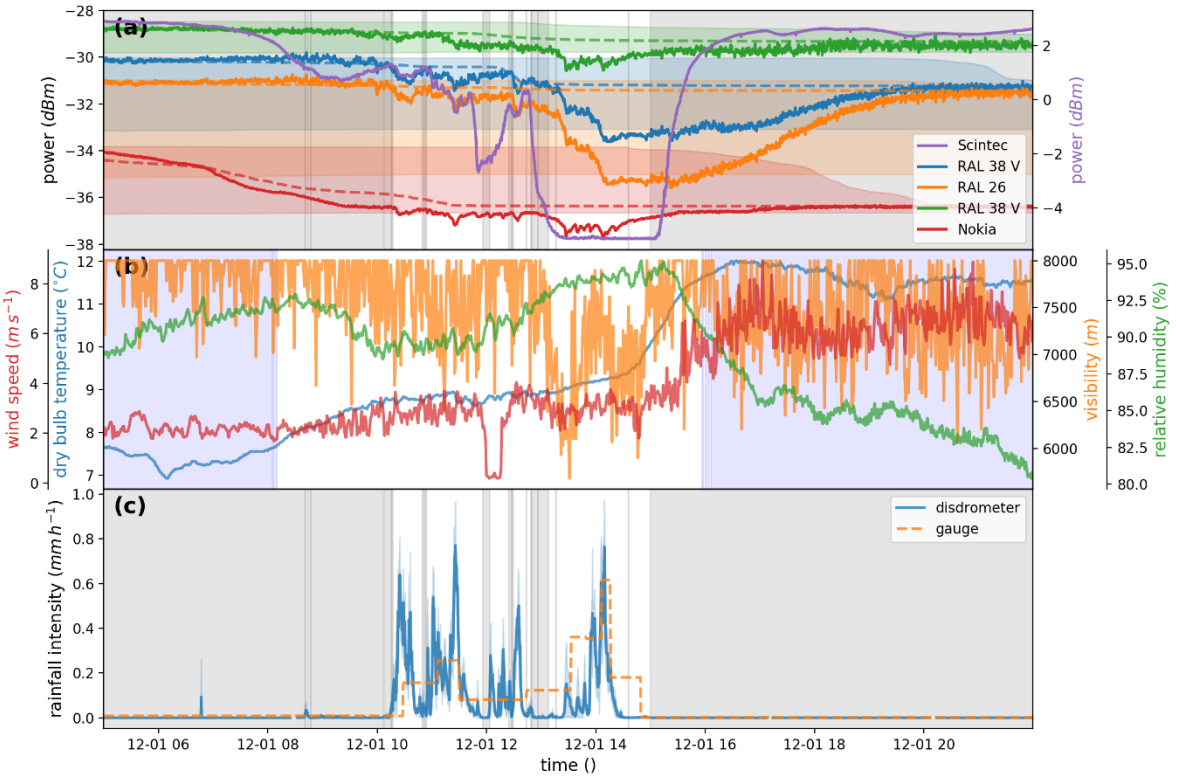

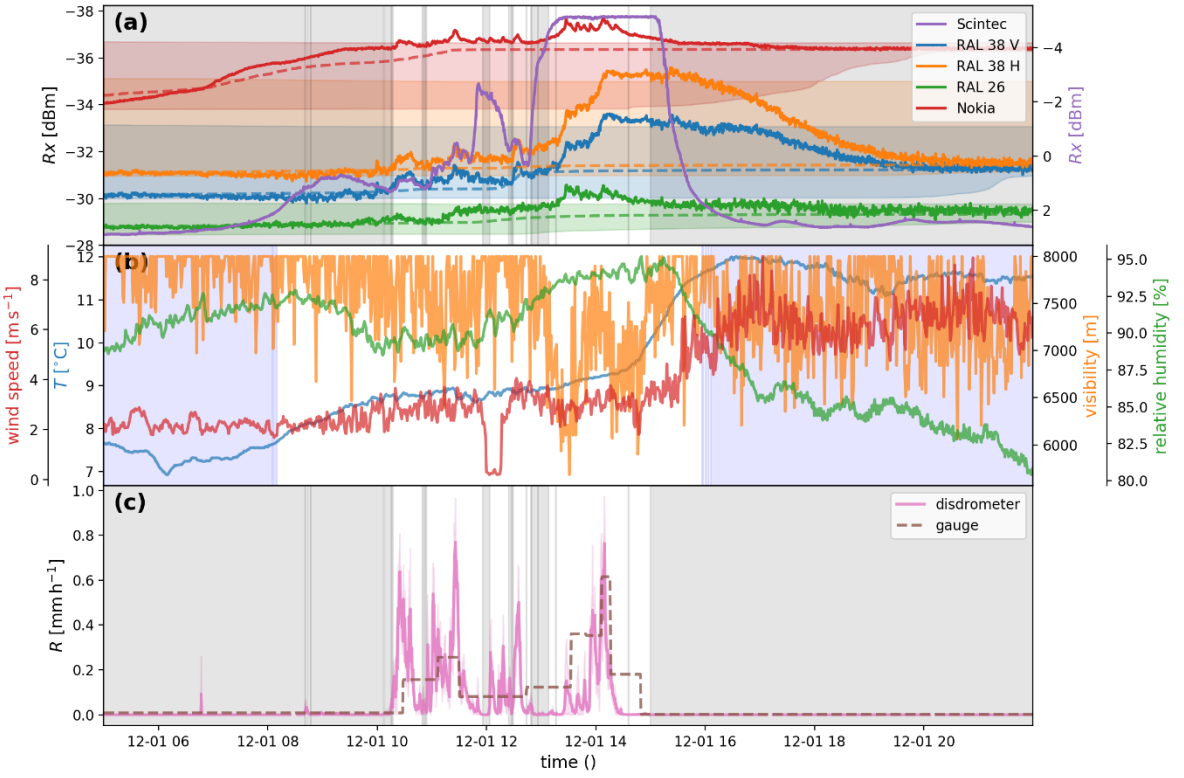

Figure 17: Time series of an event on 1 December 2015. (a): Received power levels at the detectors~~, with the~~ (solid lines) and reference levels (median over dry periods in a 24-~~-~~hour moving window) ~~indicated in darker hues.~~(dashed lines). The 5th and 95th percentile of power levels over dry periods in a 24-~~-~~hour moving window are indicated by the coloured shading. (b): Several atmospheric variables measured at the "Veenkampen" meteorological station: relative humidity, visibility, ambient air temperature at 2 m and wind speed indicated with blue, orange, green and red lines respectively. Periods with a negative net radiation flux at the surface are indicated with blue shading. (c): The spatial weighted average ~~Rainfall~~rainfall intensities derived from the disdrometers are indicated by the ~~blue~~pink line, with the weighted standard deviation among the disdrometers indicated with the ~~light blue~~pink shaded area. The

rainfall intensities derived from the tipping bucket gauge are indicated with the dashed line. Dry periods, as ~~indicated by~~determined with the disdrometers, are ~~indicated with~~represented by grey shaded areas.

Table 1: ~~results~~properties of the link antennas used in this experiment

	Nokia	RAL 38 GHz	RAL 26 GHz
Antenna diameter	300 mm	150 mm	250 mm
Antenna gain	40.1 dBi	33.0 dBi	34.5 dBi
Beam width	1.6 º	3.5 º	3.5 º

Table 2: Results of the regression of Fig. 11 applied to different subsets of the data.

	Corr. Nokia	Slope Nokia	Corr. RAL 38V	Slope RAL 38V	Corr. RAL 38H	Slope RAL 38H	Corr. RAL 26	Slope RAL 26
14—24 April	–0.800	–0.024	–0.831	–0.105	–0.920	–0.178	–0.879	–0.116
Whole set	0.019	–0.003	–0.461	–0.153	–0.565	–0.179	–0.546	–0.113
Rain only	0.011	0.004	–0.332	–0.170	–0.342	–0.170	–0.408	–0.123
Dry only	–0.072	–0.001	–0.573	–0.168	–0.716	–0.197	–0.719	–0.134

Table ~~3~~23: Coefficients and exponents (*a* and *b* parameters) of the *R*–*k* relationship derived from different sources for frequencies of ~~38GHz~~38 GHz and ~~26GHz~~26 GHz for both horizontally and vertically polarized radiation.

	a_{38H}	b_{38H}	a_{38V}	b_{38V}	a_{26H}	b_{26H}	a_{26V}	b_{26V}
This paper	3.83	1.05	4.16	1.07	7.70	0.93	8.75	0.98
Leijnse, 2010	3.35	1.02	3.70	1.05	6.72	0.91	7.79	0.95
ITU-R	2.82	1.13	3.06	1.17	5.92	1.01	6.69	1.06